AD-A065 432 AIR FORCE INST OF TECH WRIGHT-PATTERSON AFB OHIO F/G 7/3
LASER INDUCED PHOTOPHYSICS OF BIACETYL.(U)
SEP 78 T J QUELLY
UNCLASSIFIED AFIT-CI-79-88T NL

1 OF 1
AD
A065432

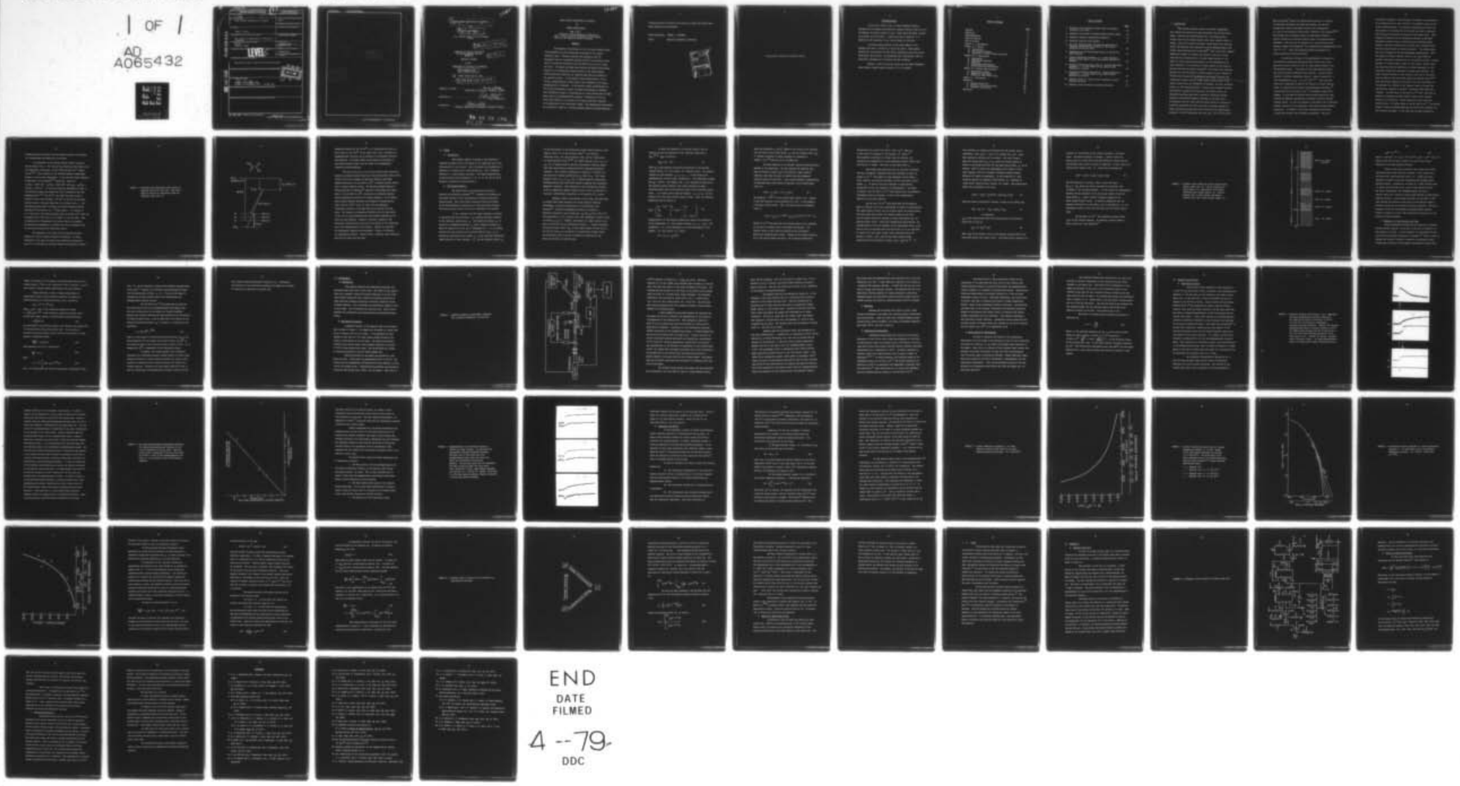

END
DATE
FILMED
4--79
DDC

AD A065432

LEVEL II

①

UNCLASSIFIED

SECURITY CLASSIFICATION OF THIS PAGE (*When Data Entered*)

REPORT DOCUMENTATION PAGE	READ INSTRUCTIONS BEFORE COMPLETING FORM
1. REPORT NUMBER CI 79-88T	2. GOVT ACCESSION NO.
3. RECIPIENT'S CATALOG NUMBER	
4. TITLE (*and Subtitle*) Laser Induced Photophysics of Biacetyl	5. TYPE OF REPORT & PERIOD COVERED Thesis
	6. PERFORMING ORG. REPORT NUMBER
7. AUTHOR(*s*) Thomas J. Quelly	8. CONTRACT OR GRANT NUMBER(*s*)
9. PERFORMING ORGANIZATION NAME AND ADDRESS AFIT student at Massachusetts Institute of Technology	10. PROGRAM ELEMENT, PROJECT, TASK AREA & WORK UNIT NUMBERS
1. CONTROLLING OFFICE NAME AND ADDRESS AFIT/CI WPAFB OH 45433	12. REPORT DATE September 1978
	13. NUMBER OF PAGES 71
4. MONITORING AGENCY NAME & ADDRESS(*if different from Controlling Office*)	15. SECURITY CLASS. (*of this report*) UNCLASSIFIED
	15a. DECLASSIFICATION/DOWNGRADING SCHEDULE

6. DISTRIBUTION STATEMENT (*of this Report*)

Approved for Public Release, Distribution Unlimited

17. DISTRIBUTION STATEMENT (*of the abstract entered in Block 20, if different from Report*)

DDC
RECEIVED
MAR 8 1979
RECEIVED
C

18. SUPPLEMENTARY NOTES

JOSEPH P. HIPPS, Major, USAF
Director of Information, AFIT 16 Feb 1979

19. KEY WORDS (*Continue on reverse side if necessary and identify by block number*)

20. ABSTRACT (*Continue on reverse side if necessary and identify by block number*)

DD FORM 1 JAN 73 1473 EDITION OF 1 NOV 65 IS OBSOLETE

UNCLASSIFIED

SECURITY CLASSIFICATION OF THIS PAGE (*When Data Entered*)

DDC FILE COPY

79-88T

(6) LASER INDUCED PHOTOPHYSICS OF BIACETYL

by

(10) THOMAS JOSEPH QUELLY

B.S., United States Air Force Academy
(1977)

(9) Master's thesis,

SUBMITTED IN PARTIAL FULFILLMENT
OF THE REQUIREMENTS FOR THE
DEGREE OF

(12) 72 p.

MASTER OF SCIENCE

at the

MASSACHUSETTS INSTITUTE OF TECHNOLOGY

(11) Sep~~tember, 19~~78

ⓒ Thomas Joseph Quelly, 1978

(14) AFIT-CI-79-88T

Signature of Author . . . . Thomas J Quelly . . .
Department of Chemistry, September 7, 1978

Certified by. . . . .
Thesis Supervisor

Accepted by . . . . G A Berchtold . . . .
Chairman, Departmental Committee on Graduate Students

79 02 28 170

012 200

79-88T

LASER INDUCED PHOTOPHYSICS OF BIACETYL

by

THOMAS JOSEPH QUELLY

MIT

Submitted to the Department of Chemistry on
Sept. 7, 1978 in partial fulfillment of the require-
ments for the Degree of Master of Science.

ABSTRACT

The emissions from biacetyl at 5-10 Torr were studied following multiphoton CO_2 laser vibrational excitation of the triplet electronic state. Biacetyl molecules are prepared in the ^3A_u metastable state by intersystem crossing from the ^1A_u electronic state which is excited by irradiation with the 4579 Å line of a c.w. argon ion laser. An intense CO_2 laser pulse excites the system vibrationally. Changes in the luminescence characteristics of the electronically excited molecules induced by the infrared laser pulse are studied in two spectral regions. In the spectral region characteristic of the $^3A_u \rightarrow {}^1A_g$ phosphorescence a decay which is fast compared to the normal phosphorescence is observed. In the spectral region characteristic of the $^1A_u \rightarrow {}^1A_g$ fluorescence a burst of delayed fluorescence is observed. This fluorescence signal is characterized by a fast risetime and the same decay time as the phosphorescence emission. Attenuation of the CO_2 laser pulse results in an increase in the decay times and a decrease in the amplitude of the fluorescence signal. The experimental observations are explained in terms of a recently proposed theory of delayed molecular fluorescence which is based on the mixing of singlet and triplet zero-order electronic configurations.

Thesis Supervisor: JEFFREY I. STEINFELD

Title: Associate Professor of Chemistry

ACCESSION for
NTIS White Section ☑
DDC Buff Section ☐
UNANNOUNCED ☐
JUSTIFICATION
BY
DISTRIBUTION/AVAILABILITY CODES
Dist. AVAIL. and/or SPECIAL
A

To My parents, Thomas and Catherine Quelly.

ACKNOWLEDGEMENTS

I would like, first of all, to thank Professor Jeffrey I. Steinfeld for his support and scientific guidance during my stay at M.I.T. In addition, my special thanks go to Dr. Itamar Burak with whom I worked very closely on this project. I would also like to thank Dr. P. G. Cummins for his assistance in the initial phases of this work.

I am particularly grateful to the other members of the basement with whom I "worked" on a day-to-day basis. These people include Drs. Fran Lussier and Tony Kotlar, Melissa Charron, Craig Jensen, Chris Reiser and Jim Long. My association with these people, both as scientific colleagues and as friends, was most rewarding.

Finally, I wish to thank the Fannie and John HERTZ FOUNDATION whose generous support made my studies at M.I.T. possible.

TABLE OF CONTENTS

Page

Abstract 2

Dedication 4

Acknowledgements 5

Table of Contents 6

List of Figures 7

Chapter I -- Introduction 8

Chapter II -- Theory 15

- A. Introduction 15
- B. The Isolated Molecule 15
- C. Molecules in a High Pressure Gas Phase 24

Chapter III -- Experimental 28

- A. Introduction 28
- B. Experimental Apparatus 28
- C. Materials 33
- D. Luminescence Measurements 33
- E. Energy Deposition Measurements 34

Chapter IV -- Results and Discussion 36

- A. Experimental Results 36
- B. Comparison with Theory 45
- C. Effects of Added Buffer Gases 60

Chapter V -- Conclusions 62

Appendices 63

- A. Variable Delay Unit 63
- B. Density of States Calculation 66
- C. Joulemeter Resurfacing 67

References 69

LIST OF FIGURES

		Page
1.	Electronic and vibrational energy levels of biacetyl relevant to this work.	12
2.	Schematic level scheme for mixed singlet-triplet states.	22
3.	Schematic diagram of experimental apparatus.	29
4.	Transient emissions from biacetyl.	37
5.	CO_2 laser induced delayed fluorescence amplitudes vs. remaining phosphorescence intensity at the time of triggering of the CO_2 laser.	40
6.	Phosphorescence and fluorescence decays at various CO_2 laser fluences.	43
7.	Inverse temperature parameter, β, vs. mean molecular energy or mean number of CO_2 laser photons absorbed per molecule.	48
8.	Biacetyl luminescence decay times vs. inverse temperature parameter, β, or mean number of CO_2 laser photons absorbed per molecule.	50
9.	Fluorescence emission amplitude vs. inverse temperature parameter, β, or mean number of CO_2 laser photons absorbed per molecule.	52
10.	Schematic model of vibronic level relaxation in high pressure gas phase.	57
11.	Schematic circuit diagram of variable delay unit	64

I. INTRODUCTION

The excited electronic states of biacetyl ($CH_3COCOCH_3$) have engaged the attention of many researchers over the past forty years. Interest has centered primarily on the lowest excited singlet state and the nearby triplet state lying slightly lower in energy. Early work involving biacetyl concentrated on the lifetime, yield, and quenching rates associated with the phosphorescence from triplet state molecules both in solution[1,2] and in the vapor phase.[3] Subsequent interest in biacetyl was related to its use as a gas phase emission standard and as a triplet energy acceptor in the study of triplet molecule participation in the photochemistry of other molecules.[4] The literature on these aspects of the study of biacetyl has been extensively reviewed.[5] More recent work involving biacetyl has used the behavior of this molecule to test theories of "radiationless transitions". Parmenter and Poland[6] observed that intersystem crossing from the lowest excited singlet state to the nearby triplet state was independent of pressure, and thus, evidently occurred in the isolated molecule. Calvert and co-workers[7] verified this behavior, measured the lifetime of the triplet state, and determined quenching rates with a variety of collision partners. McClelland and Yardley[8] measured lifetimes of the short-lived fluorescence from the lowest excited singlet state as a function of excitation wavelength and also, were able to estimate amounts of excess vibrational energy removed by collisions with cold biacetyl molecules ($\approx 730\ cm^{-1}$/collision) and with argon ($\approx 90\ cm^{-1}$/coliision).

Moss and Yardley[9] studied the phosphorescence decay as a function of excitation wavelength and added gas pressure, and saw some evidence for reverse intersystem crossing, but interpreted it as loss to the electronic ground state. Kommandeur and co-workers[10-12] have carried out an extensive series of experiments involving optical excitation to selected vibronic levels of isolated biacetyl molecules. This work will be referred to in greater detail later. Recently, Wampler and Oldenborg[13] have remeasured the phosphorescence lifetime (1.7 ±0.1 msec) and determined quenching parameters for several additional collision partners.

Of particular interest in the photophysics of biacetyl is the efficient intersystem crossing process in which some of the molecules initially excited to the ^1A_u state become trapped in the ^3A_u metastable state. The nature of this radiationless process has not been clearly understood until recently. Initial studies reported a collision independent singlet → triplet process with a rate corresponding to $k_{ST} = 7.6 \times 10^7$ sec^{-1}.[6-8] This high rate could not be explained in terms of the density of triplet vibronic states, as required by the theory of radiationless transitions.[14] A recent work by van der Werf et al.[12] has helped to solve this dilemma. In this work the authors report having carried out time-resolved fluorescence measurements on biacetyl excited to various vibronic levels. At very low pressures (a few mTorr) the fluorescence emission consisted of two components, each having the same spectral composition. In addition to the known nanosecond fluorescence, a long-lived (several μsec) emission was observed. This slow fluorescence component, termed delayed fluorescence, was accompanied by an emission with the same lifetime in the spectral region of the triplet phosphorescence. The delayed fluorescence was found to be very sensitive to pressure and its lifetime was found to decrease with increasing vibrational excitation of the singlet state. This delayed fluorescence and the accompanying emission in the phosphorescence spectral region, observed from an isolated biacetyl molecule, has been interpreted as the decay from a vibronic level which has mixed singlet and triplet character. The mixing arises due to the breakdown of the Born-Oppenheimer approximation. While the density of triplet vibronic levels is not high enough to provide a dissipative mechanism for an irreversible singlet → triplet process, it is high enough so that the real single vibronic level wave function should be described as a linear combination of the zero-order singlet and isoenergetic triplet wave functions. The width (inverse lifetime) of this vibronic level can be calculated from the widths of the zero-order singlet and triplet levels.[12,15] Since the singlet character is diluted in the real description of the molecule, the lifetime of the vibronic levels is longer than expected when viewed as a "singlet", and shorter when viewed as a "triplet". In their work van der Werf et al.[12] have been able to measure the lifetimes of these vibronic levels in the isolated molecule as a function of excess vibrational energy above the singlet origin. In another paper by van der Werf et al,[15] the authors suggest a theory of delayed molecular fluorescence for molecules in a high pressure gas phase. In our work both the data collected on isolated biacetyl molecules, and the theory pertaining to molecules in a high-pressure gas phase will be utilized.

An orientation to the relevant energy levels in biacetyl may be found in Fig. 1. The ^1A_u and ^3A_u origins are well known in the low temperature solid phase, and are 22873 and 20421 cm^{-1}, respectively.[16,17] Their location in the isolated molecule (vapor-phase spectra) is not as well established. In our work the values suggested by Kommandeur and co-workers[10,18] were used. These are, $\nu_{oo}(^1A_u) = 22300\ cm^{-1}$, $\nu_{oo}(^3A_u) = 20100\ cm^{-1}$, with $E_{ST} = \nu_{oo}(^1A_u) - \nu_{oo}(^3A_u) = 2200\ cm^{-1}$. It has been found that absorption of light in the 460-360 nm region can excite both (^1A_u) fluorescence and (^3A_u) phosphorescence.[8,12] The 4575 Å line which was used to excite biacetyl in this work lies about ~460 cm^{-1} to the red of the origin and must excite a hot-band transition, as is shown in Fig. 1. The vibrational normal modes of biacetyl have been analyzed by Sidman and McClure[19] and Durig et al.,[20] among others. Of interest to us in this work is the medium intensity band at 945-955 cm^{-1}, which can be pumped by the P(20) line [10.6 μm band] of the CO_2 laser. This is assigned as an antisymmetric CH_3 rocking mode of b_u symmetry. The normal mode frequencies of biacetyl will also be required later in calculating densities of vibrational states.

The absorption of CO_2 laser lines by biacetyl has been exploited in several "double resonance" experiments. In these experiments a CO_2 laser was used to pump vibrational transitions near 10.6 μm, and spectral intensity changes were observed in either

FIGURE 1 -- Electronic and vibrational energy levels of biacetyl relevant to this work. The assignments of several CH_3 vibrational modes are indicated, after ref. 20.

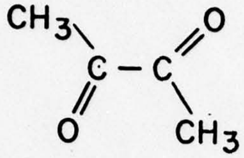
CH3
O
C – C
O
CH3

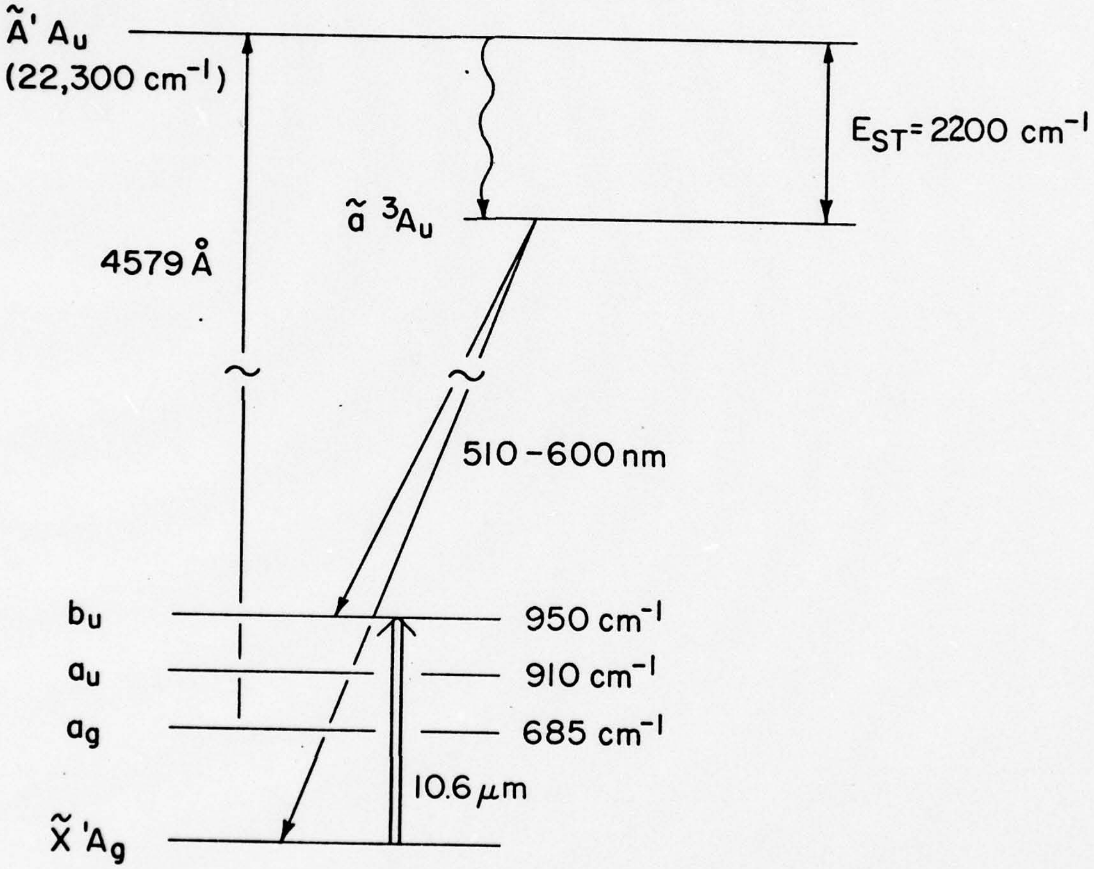
Ã' Au
(22,300 cm-1)
EST = 2200 cm-1
ã 3Au
4579 Å
510 - 600 nm
bu
au
ag
950 cm-1
910 cm-1
685 cm-1
10.6 μm
X̃ 'Ag

absorption between 510 and 435 nm[21] or in luminescence excited by a He-Cd laser at 441.6 nm.[22] In the latter work, both a diminution in phosphorescence intensity and an increase in fluorescence intensity were observed. The former effect was attributed to bleaching of the ground absorbing state, and the latter to correspondingly enhanced hot-band absorption.

The aim of this work is to use the infrared laser excitation process to prepare biacetyl molecules in high vibrational levels of the triplet state and to compare the measured lifetimes with those observed previously (van der Werf et al.[12]) by direct optical excitation to singlet vibronic levels. The recently proposed theory of delayed molecular fluorescence[15] provides a link between the experiments of van der Werf et al.[12] carried out on isolated molecules, and our experiments carried out at higher pressures. In our experiments triplet biacetyl molecules are obtained by irradiating the vapor with the 4579 Å argon ion laser line and subsequent vibrational excitation is brought about by an intense CO_2 laser pulse. The changes in luminescence induced by the CO_2 laser pulse as well as the energy deposited into the biacetyl molecules by the pulse are then measured. Chapter II contains a summary of the theoretical framework which was used in the design of this experiment and in the interpretation of the results. Chapter III describes the experimental apparatus and procedures. Chapter IV discusses our experimental results. Finally Chapter V presents some conclusions which can be drawn from this work.

II. THEORY

A. Introduction

This chapter presents a summary of the theoretical framework necessary both in the design of our experiment and in the interpretation of our results. Part B describes the photophysics of biacetyl as it applies to an isolated molecule. Part C considers molecules in a high pressure gas phase. The theory presented here is derived mainly from references 12, 14, 15, 23, 24, and 25, which should be consulted for further details.

B. The Isolated Molecule

The modern theory of intramolecular electronic coupling and relaxation processes[14,24] considers the scrambling of zero-order vibronic levels *corresponding to different electronic* configurations. This level mixing originates from the breakdown of the Born-Oppenheimer approximation or from spin-orbit coupling. The resulting mixed states are active in absorption and emission.

In its simplest form the theory considers a manifold of electronically excited states, ϕ_S, carrying oscillator strength to the electronic ground state, ϕ_O. The manifold of states, ϕ_S, is coupled to a background manifold, ϕ_ℓ, with a coupling strength $V_{S\ell}$, which for simplicity we will say is independent of ℓ. In an isolated molecule the time evolution of an excited vibronic level, ϕ_S, is essentially determined by the widths, γ_ℓ, of the zero-order background levels relative to their spacings, ρ_ℓ^{-1}, and the energetic width, $\Delta_{S\ell}$, of the distribution of the effectively coupled levels relative to the spectral width, ΔE, of the exciting light.[15] Two limiting situations arise, the "small molecule" limit and the "statistical" or "large molecule" limit.[24,25] The "small molecule" limit ($\gamma_{\ell}\rho_{\ell} < 1$, $\Delta_{s\ell} > \Delta E$) is characterized by observed fluorescence lifetimes longer than those which would be expected from the integrated absorption intensity. This lifetime lengthening is caused by a "dilution" of the oscillator strength carried by the ϕ_s level to ϕ_o. The "large molecule" limit ($\gamma_{\ell}\rho_{\ell} > 1$, $\Delta_{s\ell} < \Delta E$) is characterized by fluorescence lifetimes shorter than those which would be expected from integrated absorption intensity. This shortening of the fluorescence lifetime is due to competition between radiative decay of the ϕ_s state and irreversible radiationless transitions to the manifold of ϕ_{ℓ} states.

Biacetyl, which is the subject of this study, has been shown to exhibit both "small molecule" and "large molecule" behavior. Accordingly, it has been classified as an "intermediate case" molecule.[12] Biacetyl's photophysical behavior is typical of molecules containing a small energy gap ($\nu_{oo}(^1A_u)-\nu_{oo}(^3A_u) = 2200\ \text{cm}^{-1}$). The interaction of a ^1A_u vibronic level with isoenergetic triplet levels is strong ($\rho_T V_{ST} > 1$). However, the density of triplet levels is too small to provide a facile radiationless singlet → triplet transition. The ground singlet state, ^1A_g, is only weakly coupled to both the ^1A_u and the ^3A_u states, but the density of ground state vibronic levels is sufficiently high to provide a dissipative continuum for the decay from singlet or triplet levels.

To treat the dynamics of an excited vibronic level of biacetyl we used the formalism of the "effective Hamiltonian", H_{eff}.[23,27] H_{eff} is given by,

$$H_{eff} = H_M - i\gamma/2 \qquad (1)$$

where H_m is the molecular interaction Hamiltonian of the strongly coupled singlet, $|S\rangle$, and triplet, $|T\rangle$, vibronic levels. Its diagonal elements are the energies, ε_S, ε_T, $\varepsilon_{T'}$, ..., of the singlet and quasidegenerate triplet levels, respectively. Its nondiagonal elements are $V_{ST} = \langle S|V|T\rangle$. The damping term, $-i\gamma/2$, provides the coupling of the strongly coupled subspace, with other continuous or quasi-continuous media such as the radiation field or the electronic ground state. $\underset{\sim}{\gamma}$ is a matrix whose diagonal elements, γ_S, γ_T, $\gamma_{T'}$, are the widths of the zero order coupled vibronic levels. Thus, the effective Hamiltonian can be written as

$$H_{eff} = \begin{pmatrix} \varepsilon_S - i\gamma_S/2 & V_{ST} & \cdots & V_{ST'} \\ V_{ST} & \varepsilon_T - i\gamma_T/2 & \cdots & 0 \\ \vdots & \vdots & & \vdots \\ V_{ST'} & 0 & \cdots & \varepsilon_{T'} - i\gamma_{T'}/2 \end{pmatrix} \qquad (2)$$

Diagonalization of the effective Hamiltonian leads to the formation of new eigenstates, $|n\rangle$, with complex energies, $E_n = \varepsilon_n - i\gamma_n/2$. The eigenstates, $|n\rangle$, can be expressed as a linear combination of the singlet, $|S\rangle$, and triplet, $|T\rangle$, levels,

$$|n\rangle = \alpha_n |S\rangle + \sum_T \beta_n^T |T\rangle \qquad (3)$$

where the parameters α_n and β_n^T depend on the triplet level spacings, the zero-order triplet decay widths, γ_T, and the coupling terms, V_{ST}. A complete discussion of these parameters is contained in Lahmani, et al.[23] and will not be included here.

The time evolution of an isolated, excited biacetyl molecule depends on its preparation. We will consider the idealized case when the biacetyl singlet state is excited by a short pulse of radiation, such that the pulse is shorter than any subsequent evolution time of the molecule. Such a pulse prepares a superposition of quasistationary states which is identical to the nonstationary state $|S\rangle$:

$$|\phi(0)\rangle = \sum_n \alpha_n |S\rangle = |S\rangle = \sum_n A_n |n\rangle \tag{4}$$

The operation $e^{-iH_{eff}\,t}$ on an initial state vector $|\gamma(0)\rangle$ results in the time evolution of the projection of $|\gamma(t)\rangle$ on the subspace of strongly coupled states. Thus, the state vector at subsequent times is,

$$|\gamma(t)\rangle = \sum_n A_n \; |n\rangle \; e^{-iE_n t} = \sum_n A_n \; |n\rangle e^{-i\varepsilon_n t} \; e^{-\gamma_n \, t/2} \tag{5}$$

Lahmani, et al.[23] has shown that the resulting decay can be expressed as the sum of a coherent and an incoherent contribution. The coherent decay is very rapid and represents the interference between the quasistationary states. Because of the sudden excitation all of the initial phases are equal. The resulting constructive interference will persist for about a time Δ_{ST}^{-1}, where Δ_{ST} is the spread in frequency of the decaying $|n>$ levels.[12] The incoherent contribution is slower than the coherent, and represents the superposition of slow exponential decays arising from the various $|n>$ states, each with its own decay width γ_n.

The average decay characteristics of the short (coherent) and long (incoherent) components have been discussed in detail by Lahmani, et al.[23] They depend on such parameters as the triplet level spacing, the coupling strengths, and the zero-order triplet widths, γ_T. In general the short component is approximately exponential and the long component is nonexponential. As stated in Chapter I, van der Werf, et al.[12] have observed this two-component fluorescence decay in biacetyl, as well as the nonexponential character of the slow component.

Van der Werf, et al.[12] have shown that the fluorescence decay of biacetyl can be well approximated in terms of a biexponential. This approximation assumes that the triplet levels are evenly spaced, they have equal decay widths, all coupling terms are the same, and the singlet oscillator strength is evenly distributed over the quasistationary states. Using this biexponential approximation, the average widths of the slow component of the fluorescence decay, $\gamma_n(E)$, which we will be concerned with from this point on, can be expressed in terms of the zero order triplet levels characterized by the density of states, $\rho_T(E)$, and the zero-order singlet levels characterized by the density of states, $\rho_S(E) = \sum_S \delta(E-E_S)$.[15] In this treatment all energies are measured from the triplet origin. Furthermore, since $\rho_S(E) << \rho_T(E)$ it is assumed that $\rho_n(E) \approx \rho_T(E)$. Three physical situations are of interest. The first, range A, spans the energy region $E_{S_O} \leq E \leq E_\alpha$, where the singlet density of states is low enough such that the zero-order decay widths, γ_S, do not overlap. Each $|S>$ state acts independently with regard to interstate coupling, while off resonance intrastate coupling between different $|S>$ states is negligible. In this range the $|n>$ level structure consists of regions of mixed states, $|n>$, separated by "black holes" containing pure triplet, $|T>$, states. The average decay widths can be expressed in the form,

$$\gamma_n(E_n) = \gamma_T(E_n) + \sum_S \theta(E_n - E_S)\ \gamma_S(E_S)/\Delta_{ST}\ \rho_T(E_S) \qquad (6)$$

where the singlet distribution function is taken in the simple form

$$\theta(E_n - E_S) = 1, \quad -\tfrac{1}{2}\Delta_{ST} < (E_n - E_S) < \tfrac{1}{2}\Delta_{ST} \qquad (7)$$

$$= 0, \text{ otherwise}$$

Δ_{ST} is the radiationless width which characterizes the interstate mixing and is given by,

$$\Delta_{ST} = 2\pi\ |V_{ST}|^2\ \rho_T(E) \qquad (8)$$

where $|V_{ST}|$ is the absolute value of the coupling strength between the zero-order singlet and triplet levels. The second term in equation (6) accounts for the dilution of the singlet character in the mixed state. The second situation of interest, range B, spans the energy range $E>E_\alpha$ where due to the high density of states interference between close lying $|S>$ states is important. In this region the average decay widths of the $|n>$ levels can be expressed by

$$\gamma_n(E) = \gamma_T(E_n) + \gamma_S(E_n)\ \rho_S(E_n)/\rho_T(E_n) \qquad (9)$$

The last situation of interest, range C, spans the region $E_{T_O} \leq E < E_{S_O}$, which can only be populated by collisions (and is absent in the isolated molecule). In this region the independently decaying levels correspond to the zero-order triplet levels with decay widths γ_T. Figure 2 shows a schematic diagram of the mixed singlet-triplet states. It should be emphasized that the dominant contribution to the widths $\gamma_n(E)$ is nonradiative, i.e. the luminescence yield is much less than unity over the entire energy range

Van der Werf, et al.[12] have measured the decay widths $\gamma_n(E)$ of the isolated molecule. An empirical relation based on their results has been suggested,[15]

FIGURE 2 -- Schematic level scheme for mixed singlet-triplet states, (after ref. 15). Range A consists of mixed states, $|n>$, separated by "black holes" containing pure triplet states, $|T>$. Range B consists only of mixed states, and Range C contains pure, zero -order triplet states, $|T>$.

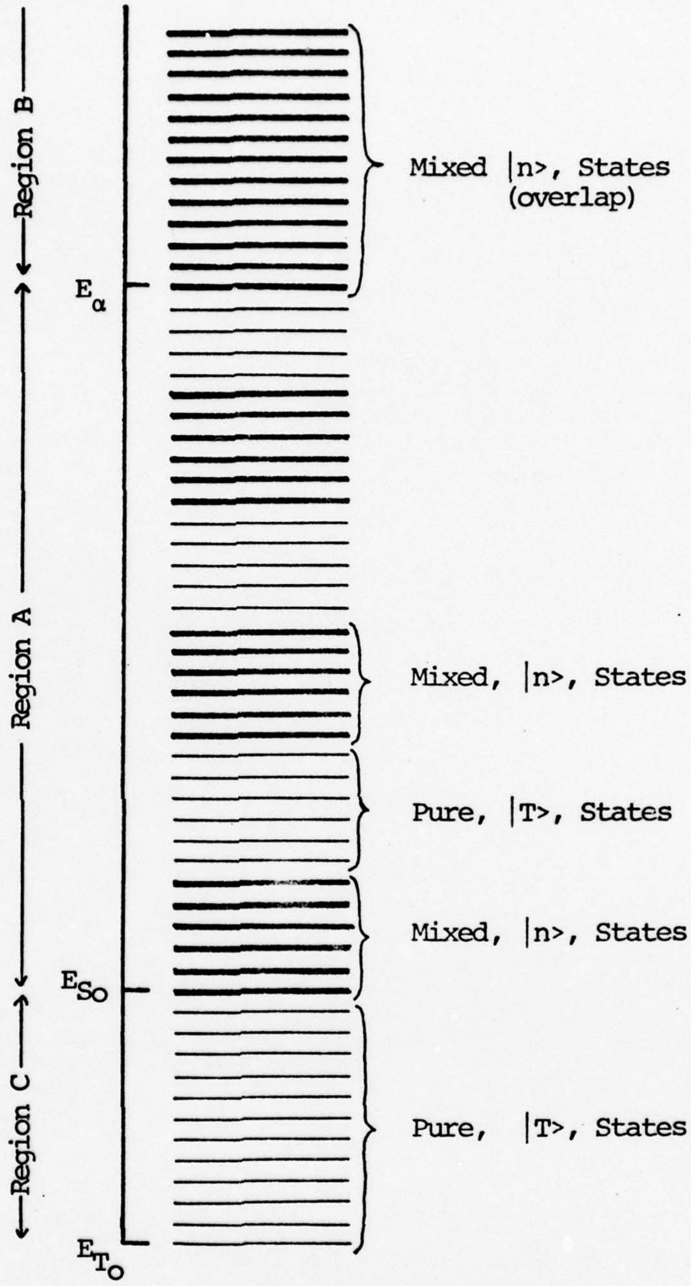
Region B
Region A
Region C
E_α
E_{S_O}
E_{T_O}
Mixed |n>, States (overlap)
Mixed, |n>, States
Pure, |T>, States
Mixed, |n>, States
Pure, |T>, States

$$\gamma_n(E) = A\ ^{BE} + C \qquad (10)$$

where $A = 300\ \text{sec}^{-1}$, $B = 1.26 \times 10^{-3}\ (\text{cm}^{-1})^{-1}$, and $C = \gamma_T^{rad} = 82\ \text{sec}^{-1}$. These results will be used to predict the decay from biacetyl molecules in the high pressure gas phase.

Since, in the case of biacetyl, both singlet and triplet zero-order states carry oscillator strength to the ground state, the decay from a quasistationary state, $|n>$, should also carry oscillator strength in both the fluorescence and phosphorescence spectral regions. Furthermore, the decay of a single vibronic level $|n>$ should yield the same value, $\gamma_n(E)$, in both spectral regions. The terms "fluorescence" and "phosphorescence" now carry a spectral definition, instead of being associated with a characteristic emission lifetime. As previously mentioned, van der Werf, et al.[12] have observed this vibronic level decay in both spectral regions following excitation of the singlet electronic manifold. Similarly, emission in both the fluorescence and phosphorescence spectral regions is expected to occur, when vibrational excitation is in the triplet electronic manifold.

C. Molecules in a High Pressure Gas Phase

Having discussed the preparation and decay of an isolated, excited biacetyl molecule, we now turn to the case of biacetyl in a high pressure gas phase. In this treatment two assumptions concerning the molecule-medium interaction are required.[15] First, it must be assumed that thermal vibrational relaxation and excitation rates considerably exceed all of the relevant intramolecular decay rates.

Second, the widths of the resonances are considerably lower than the thermal energy, $\beta^{-1} \equiv kT$, in the temperature range of interest, $(\beta\gamma_n << 1)$. This implies a uniform thermal distribution with each resonance.

Under conditions in which a thermal distribution is established within an excited vibronic manifold, the number of excited molecules at a particular energy, n(E), is given by,

$$n(E) = Z^{-1} N e^{-\beta E} \rho_n(E)$$

where $\rho_n(E) = \rho_T(E)$ is the vibrational density of states, $Z = \int_0^\infty dE\, \rho_n(E)\, e^{-\beta E}$ is the vibrational partition function, and N is the total number density of electronically excited molecules

$$N = \int_0^\infty n(E)\, dE \tag{12}$$

As established in the previous section, each vibronic level decays with its characteristic average decay width $\gamma_n(E)$. For the case of incoherently excited vibronic levels (as would be the case in a high pressure, thermalized system),

$$\frac{dn(E)}{dt} = -\gamma_n(E) n(E) \tag{13}$$

From equations (11)-(13) it follows that

$$\frac{dN}{dt} = -N <\gamma> \tag{14}$$

where

$$<\gamma> = Z^{-1} \int_0^\infty \gamma_n(E)\, \rho_n(E)\, e^{-\beta E}\, dE \tag{15}$$

Thus, in a high pressure gas phase the macroscopic (observable) decay rate, $\langle\gamma\rangle$, can be expressed in terms of the thermally averaged decay rates $\gamma_n(E)$.[15] Equation (15) provides a quantum mechanical result for the experimental lifetime, τ_p, ($\langle\gamma\rangle = 1/\tau_p$) for the decay of vibronically excited molecules both in the fluorescence and phosphorescence spectral regions.

Van der Werf et al.[15] have shown that the ratio of the fluorescence yield to the phosphorescence yield depends upon the level of excitation in the singlet (or triplet) manifold. Adopting the procedure developed by these authors for the calculation of radiative decay rates, it can be shown that the intensity of the delayed fluorescence emission, I_F, is related to β according to the expression,

$$I_f = \frac{1}{3} N \gamma_s^{rad} e^{-\beta E_{ST}} \tag{16}$$

where N is the number of vibronically excited molecules, E_{ST} is the energy separation of the singlet and triplet origins, and γ_s^{rad} is the radiative width of the zero-order singlet vibronic levels. It is assumed that γ_s^{rad} is independent of the vibrational energy.

In summary, this theory predicts that vibrational excitation of a previously prepared, thermal system of triplet state biacetyl molecules in a high pressure gas phase will result in the formation of excited vibronic levels containing both singlet and triplet character. Emission from these mixed levels will occur in both the fluorescence and phosphorescence spectral regions and will have a decay lifetime determined by equation (15). Furthermore, the intensity of the fluorescence emission will depend on the degree of excitation as expressed in equation (16).

III. EXPERIMENTAL

A. Introduction

This chapter describes the experimental apparatus and procedures which were used in this study. The object of this experiment was to prepare a system of biacetyl molecules in the ^3A_u state using optical excitation and to observe the emission properties of these molecules following vibrational excitation induced by pulsed infrared radiation. Part B describes the experimental apparatus used in this study. Part C describes the materials used. Parts D and E describe the luminescence and energy deposition measurements, respectively.

B. Experimental Apparatus

A schematic diagram of the apparatus used in this experiment is shown in Figure 3. The sample cell consisted of a pyrex tube, 22 mm in diameter and 20 cm in length. It was equipped with NaCl windows at each end and a 90° pyrex viewing window located at the region of intersection of the two beams. The sample was admitted directly from a vacuum system, with pressures measured on a Wallace & Tiernan direct-reading dial gauge. The vacuum system was capable of achieving pressures as low as 5 mTorr between runs.

Optical excitation of the sample was provided by a CR6 Argon ion laser. Input power was approximately 150 mW at 4579 Å. The visible beam was approximately collimated with a beam diameter of about 2 mm in the viewing region. Infrared pulsed excitation was provided by a Tachisto 215G TEA-CO_2 laser (P(20), 10.6 μm branch). This laser is

FIGURE 3 -- Schematic diagram of experimental apparatus. For a detailed explanation, see the text.

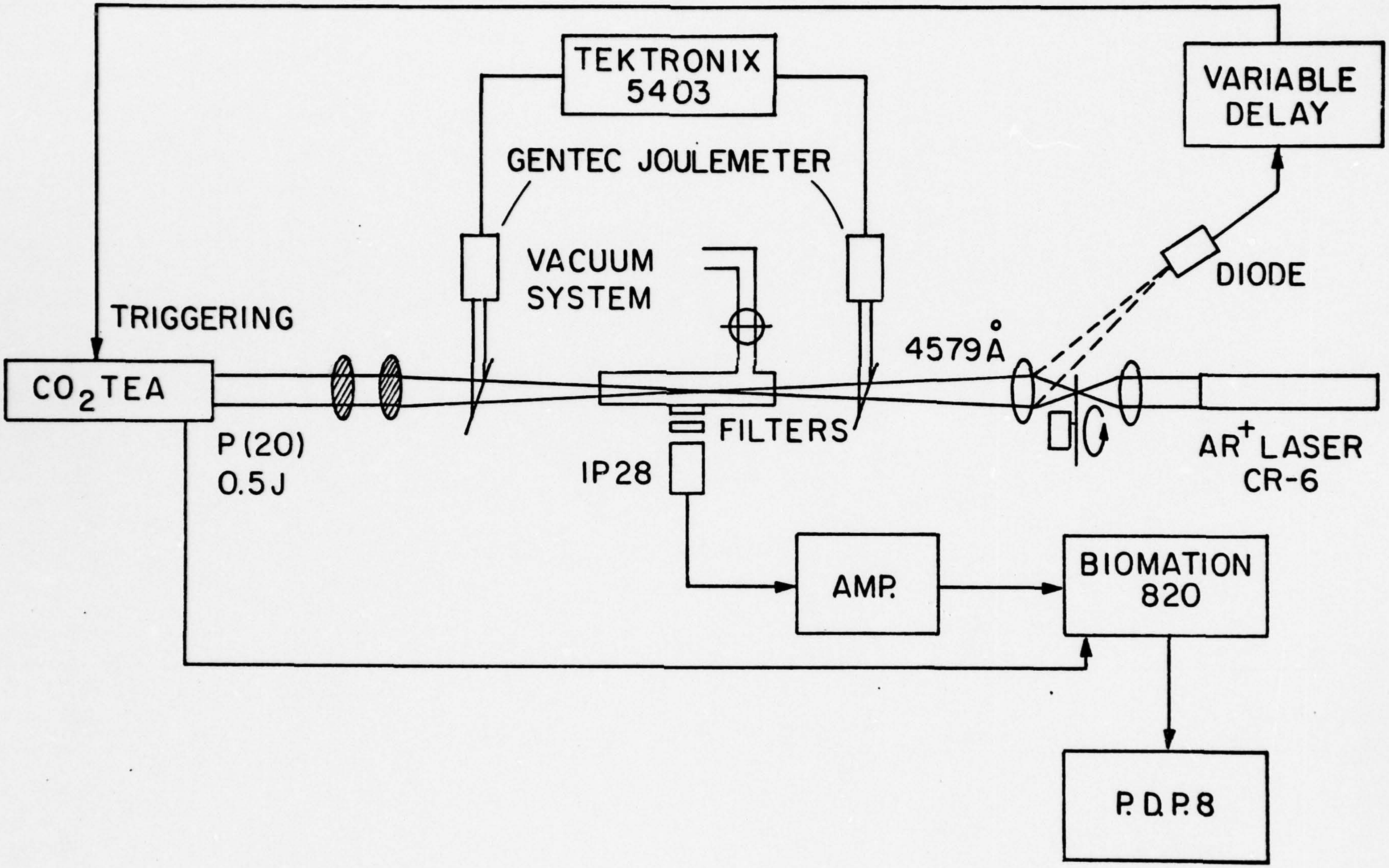
TEKTRONIX
5403
VARIABLE
DELAY
GENTEC JOULEMETER
VACUUM
SYSTEM
DIODE
TRIGGERING
4579Å
CO_2 TEA
FILTERS
P (20)
0.5 J
IP28
AR$^+$ LASER
CR-6
AMP.
BIOMATION
820
P. D. P. 8

nominally capable of delivering .5 J TEM_{00} per pulse. The pulse consists of a 40 nsec (FWHM) gain-switched spike followed by a 500 nsec tail, with about two thirds of the energy contained in the spike. The infrared beam was brought to a soft focus in the center of the viewing region by means of a variable focal length telescope. The telescope consisted of two AR-coated Ge lenses (II-VI, Inc.), a plano-convex ($f\ell$ = 28.27 cm) and a plano-concave ($f\ell$ = -28.27 cm). The two beams were counter-propagating and were carefully aligned to insure maximum overlap in the viewing region.

A ZnSe beamsplitter was placed between the telescope and the sample cell with its vertical axis perpendicular to the direction of propagation of the infrared beam. This beamsplitter split off about 5% of the infrared beam which was detected by a Gentec ED-200 pyroelectric joulemeter. Calibration of this beamsplitter permitted constant monitoring of the infrared pulse energy. A second beamsplitter made of BaF_2 was placed after the sample cell. It split off about 5% of the transmitted infrared beam which was detected by a second Gentec ED-200 joulemeter. The BaF_2 beamsplitter, placed with its horizontal axis perpendicular to the direction of propagation of the infrared beam, passed the visible beam (vertically polarized) with little attenuation, but blocked most of the infrared beam (horizontally polarized) to prevent damage to the glass optics by the infrared pulses. The signals from the two Gentec joulemeters were displayed on a Tektronix 5403 dual-trace oscilloscope.

The infrared energy reaching the sample cell was controlled by an attenuation cell (not shown in Figure 3) placed between the CO_2

laser and the telescope. The cell consisted of a pyrex tube, 22 mm in diameter and 8 cm in length, with NaCl windows mounted at Brewster's angle on each end. The cell was filled with 0-8 Torr of SF_6 depending on the degree of attenuation desired.

For reasons which will be described in Chapter IV, it was necessary to fire the infrared laser at a controlled delay following shut-off of the visible exciting light. This was accomplished by focussing the Ar^+ laser beam into the plane of a mechanical chopper blade, giving a 5 μsec cut-off time. A portion of the beam reflected from a glass lens behind the chopper was refocussed onto a phototransistor. The drop in signal when the visible light was chopped off triggered a variable delay unit (see Appendix 1), which in turn triggered the CO_2 laser. The variable delay unit was capable of delays from 1.6 - 780 μsec in two ranges.

Emission from the interaction region was detected by an RCA 1P28 photomultiplier. A combination of interference filters (Ditric Optics Inc. or Optics Technology Inc.) were used to isolate various portions of the spectrum. A long pass filter, passing wavelengths greater than 530 nm was used to view the "phosphorescence" region. A 470 - 530 nm bandpass filter in combination with a 500 nm cut-off short pass filter allowed viewing of the "fluorescence" region. This latter filter combination passed a small amount of scattered 4579 Å light, but since all measurements were made at least 50 μsec following the cut-off of the visible beam by the chopper this posed no problems. This filter combination also passed a small amount of "phosphorescence" which was subtracted out when analyzing the "fluorescence" signals.

The signals from the photomultiplier were amplified with a wide band (Tektronix 1121, 5Hz - 17 MHz, 40db gain) amplifier, and recorded on a Biomation 820 transient recorder. A signal from the CO_2 laser was used to trigger the transient recorder. The Biomation 820 was interfaced with a PDP-8/L computer for signal averaging or processing. Averaged signals from the PDP-8/L could be stored on paper tape for further analysis or plotted on a Hewlett-Packard 2D-2A X-Y recorder.

C. Materials

Biacetyl was purchased from Fluka AG, puriss. grade, and was transferred to the sample cell following several freeze-pump-thaw distillations. Argon was taken from a Matheson Research Grade lecture bottle (purity 99.9995%), and ethane was Matheson chemically pure grade (99.5%, less than 10 ppm O_2).

D. Luminescence Measurements

Luminescence experiments were carried out at biacetyl pressures of 5 and 10 torr and at added gas pressures of 0-100 torr. In this pressure range, all emission prior to the arrival of the CO_2 laser pulse occurs from triplet molecules having a thermal vibrational distribution with a temperature of 300°K. Electronic quenching by biacetyl itself or by added dilutents such as argon or ethane is negligible.[6,7a, 8] At these pressures, the diffusion length of the metastable triplet is less than 1 mm.[28] The optical absorption coefficient at 4579 Å is unsaturated and independent of pressure under our conditions.[10] These conditions are, of course, much different from the isolated molecule studies of van der Werf et al.[12]

The primary focus of the luminescence studies was the measurement of the amplitudes and decay times of the infrared laser induced emission features in both the fluorescence and phosphorescence spectral regions, as a function of infrared pulse energy. These measurements were made primarily at biacetyl pressures of 5 torr with some measurements made at 10 torr. Additional experiments, more qualitative in nature, were made to determine the effects of added nonabsorbing diluent gases on the luminescence features of biacetyl. The amplitude and decay times of the biacetyl luminescence were measured from photographs of the Biomation 820 display screen, or directly from digital readouts associated with this instrument. More precise measurements were obtained by signal averaging. Luminescence signals resulting from infrared pulses of constant energy were averaged on the PDP-8/L computer and the results were fit[29] to an exponential curve.

E. Energy Deposition Measurements

In order to interpret the results of the luminescence measurements for this system it was necessary to know the mean vibrational excitation per molecule, i.e. the amount of infrared energy deposited in the sample. Since this is a function of both incident laser fluence, and pressure of biacetyl and diluent (if any) this had to be determined over the entire range of operating conditions. Energy deposition experiments were carried out by direct transmission, simultaneously with the luminescence measurements. This was accomplished by means of the beamsplitters and joulemeters placed before and after the sample cell, as previously described.

The calibrated beamsplitter placed before the sample cell provided an absolute measurement of the infrared energy per pulse incident to the sample cell. The transmittance (1-absorption) of the sample was measured as the ratio of the transmitted energy to the incident energy when the cell contained biacetyl divided by the same ratio when the cell was empty. The infrared beam profile was determined with a scanning 0.1 mm pinhole both at the beam waist (viewing region) and 10 cm from the beam waist. The beam was found to be multimode and the distance between the 20% intensity points was defined as the effective diameter of the beam. This distance was 3.1 mm.

The number of infrared photons absorbed per molecule is thus given by,

$$\langle n \rangle = \frac{A\eta_o}{\pi r^2 \rho} \qquad (17)$$

where A is the measured absorbance per cm, η_o is the total incident energy per pulse [photons = Joules x (1 x 10^7 ergs/Joule) x $(5.0358 \times 10^{15}\ \frac{\mathrm{cm}^{-1}}{\mathrm{erg}}) \times (944.2\ \frac{\mathrm{cm}^{-1}}{\mathrm{photon}})^{-1}$], r is the effective radius of the infrared beam, and ρ is the number density of biacetyl molecules per cm^3. Some optoacoustic measurements were also made[30], and the signal amplitude for a given sample pressure was found to be linear in laser fluence.

IV. RESULTS AND DISCUSSION

A. Experimental Results

The principal effect observed in these experiments is that the CO_2 laser pulse induces a decrease in the phosphorescence emission ($\lambda > 530$ nm) which is fast compared to the normal triplet decay time. At the same time, a burst of "delayed fluorescence" appears in the 470-500 nm region. Similar results were previously reported by Orr,[22] and interpreted as double resonance effects. Figure 4 (top) shows the signal induced by the CO_2 laser pulse when the system is exposed simultaneously to both the infrared and the visible laser beams. A fast (μsec) decrease in the phosphorescence intensity is observed, followed by a slow recovery of the emission to its initial steady state value. This signal was interpreted[22] as arising from a depletion, induced by CO_2 laser pumping, of the low-lying vibrational levels of the ground electronic state which are coupled to the visible radiation. As a result, the excitation mechanism is suddenly shut off, and the phosphorescence intensity drops. This explanation is untenable, however, since the population in the phosphorescing triplet state is unable to respond to a sudden change in the rate of feeding into that state in a time shorter than its characteristic lifetime, which is ~1.7 msec.

An alternative interpretation, adopted by us, is that the observed decay times are the result of vibrational excitation of triplet biacetyl molecules. The function of the visible laser beam is only to prepare an initial population of

FIGURE 4 -- Transient emissions from biacetyl. (Top; 2msec/div) Transient phosphorescence decrease induced by CO_2 laser pulse during cw excitation at 4579 Å. In this and the following, luminescence intensity increases downwards. (Middle; 200 μsec/div). Phosphorescence decay in biacetyl excited at 4579 Å (a) Normal decay following cut-off of excitation at [1]; (b) rapid decay following absorption of CO_2 laser pulse at [2]. (Bottom; 10 μsec/cm) Expanded view of transient region. (a) Rapid phosphorescence decay; (b) simultaneous delayed fluorescence pulse.

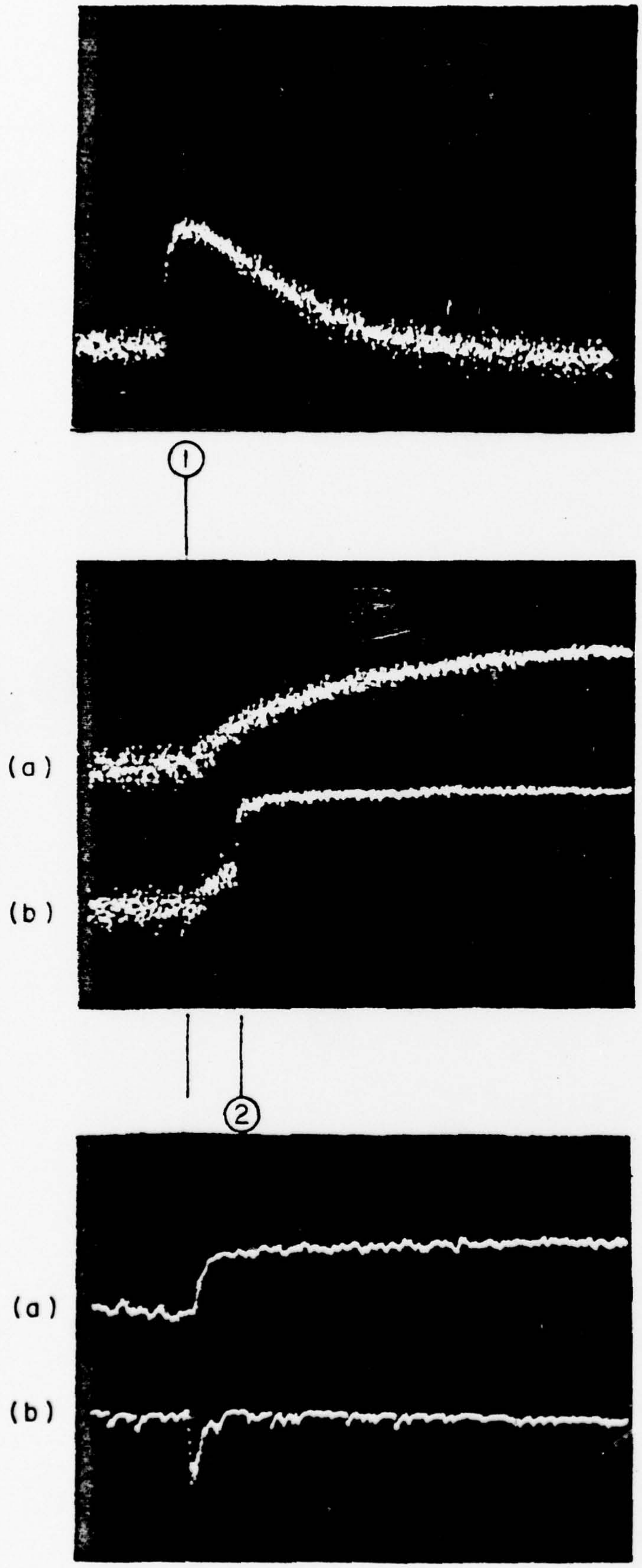
①
(a)
(b)
②
(a)
(b)

biacetyl molecules on the metastable triplet state. In order to support this interpretation, the CO_2 laser was fired at a controlled delay after the mechanical shut-off of the visible beam. Figure 4 (middle) shows the unperturbed phosphorescence decay curve (a) and a decay curve suddenly interrupted by a CO_2 laser pulse (b). The fast decay of the phosphorescence is induced by the CO_2 laser irrespective of the presence of the visible beam. Figure 4 (bottom) shows the phosphorescence signal (a) on an extended time scale, in which a decay time of several μsec can be seen. Trace (b) shows the induced fluorescence signal. It is characterized by a fast rise time, and the same decay time as the corresponding phosphorescence signal. The fact that the delayed fluorescence signal is obtained in the absence of any visible exciting light excludes the possibility that this is a normal fluorescence signal originating from optical excitation of vibrationally activated biacetyl molecules. In order to verify that the fluorescence and phosphorescence signals are directly connected to the biacetyl triplet population, the delay between the cut-off of the optical excitation and the triggering of the CO_2 laser was scanned across the phosphorescence lifetime. As shown in Figure 5, the delayed fluorescence amplitude is linearly proportional to the phosphorescence intensity remaining just prior to the arrival of the infrared pulse (where the energy per infrared pulse was held constant). This shows that it is the triplet-state molecules themselves which are responsible for the observed transients. Since the electronically unexcited biacetyl molecules are no longer

FIGURE 5 -- CO_2-laser-induced delayed fluorescence amplitudes vs. remaining phosphorescence intensity at the time of triggering of the CO_2 laser. The point at the origin corresponds to the CO_2 laser being fired after a delay of many phosphorescence lifetimes, or in the absence of the 4579 Å exciting radiation.

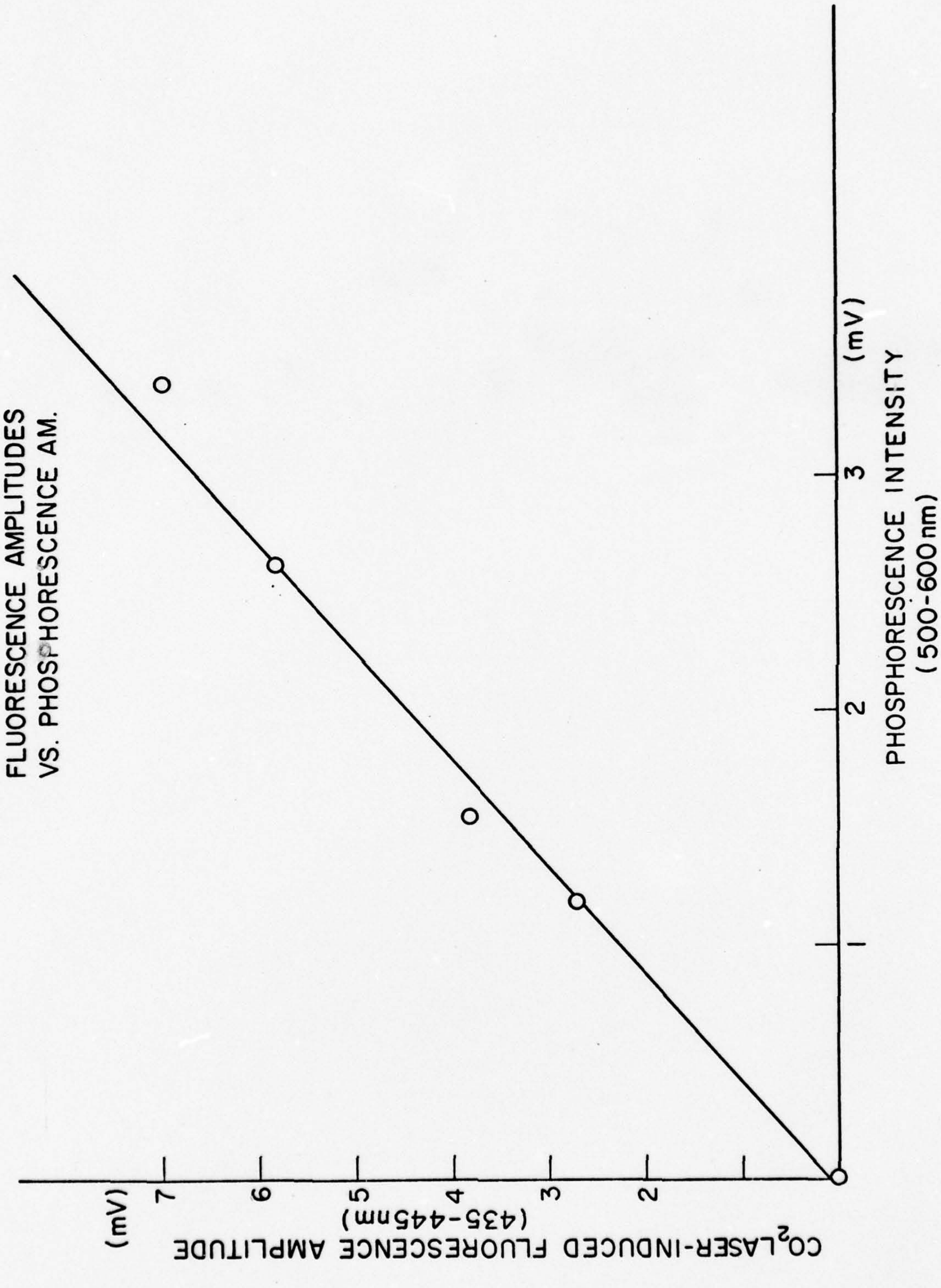
FLUORESCENCE AMPLITUDES
VS. PHOSPHORESCENCE AM.
CO$_2$ LASER-INDUCED FLUORESCENCE AMPLITUDE
(435-445nm)
(mV)
2
3
4
5
6
7
PHOSPHORESCENCE INTENSITY
(500-600nm)
(mV)
1
2
3

optically coupled to the emitting states, any change in their vibrational energy distributions should have no direct effect on the luminescence intensities. The term "delayed fluorescence", as suggested by Parker,[31] accurately describes this fluorescence emission originating from triplet states.

Having established that the delayed fluorescence and phosphorescence were the result of vibrational excitation of the triplet state biacetyl molecules, the decays in both regions were analyzed and found to be approximately exponential over two lifetimes. The lifetimes reported in this work are the result of fitting the observed decays to an exponential curve or equivalently, they represent the time required for the emission intensity to fall to 1/e times its initial value.

The characteristic features of these observations can be summarized as follows:

1. The decay times of both the phosphorescence and the delayed fluorescence signals, at the same CO_2 laser fluence and sample pressure, are equal. This is shown qualitatively in Figure 6 which shows the phosphorescence and delayed fluorescence decays at three different CO_2 laser fluences.

2. The decay times become longer as the infrared fluence diminishes. This is also shown qualitatively in Figure 6. Figure 8 shows the decay times as a function of the average number of CO_2 laser photons absorbed per biacetyl molecule.

3. The amplitude of the fluorescence signal

FIGURE 6 -- Phosphorescence and fluorescence decays at various CO_2 laser fluences. In each panel the luminescence intensity decreases downwards. The upper scan in each panel shows the phosphorescence decay, while the lower scan shows the corresponding fluorescence emission. The vertical scales are not necessarily the same in both the upper and lower scans. (Top: 10μsec/div) 4.64 CO_2 laser photons absorbed per molecule ($<1> = 944.2 cm^{-1}$); (middle, 10μsec/div) 3.73 CO_2 laser photons absorbed; (bottom; 20μsec/div) 2.36 CO_2 laser photons absorbed.

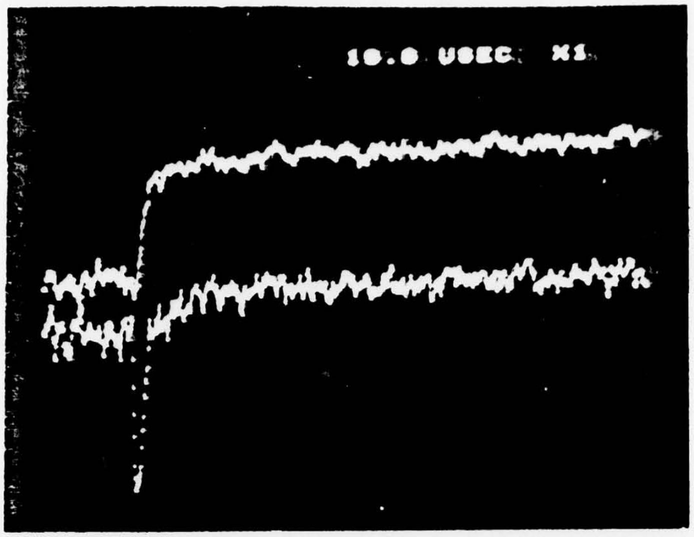
10.0 USEC X1

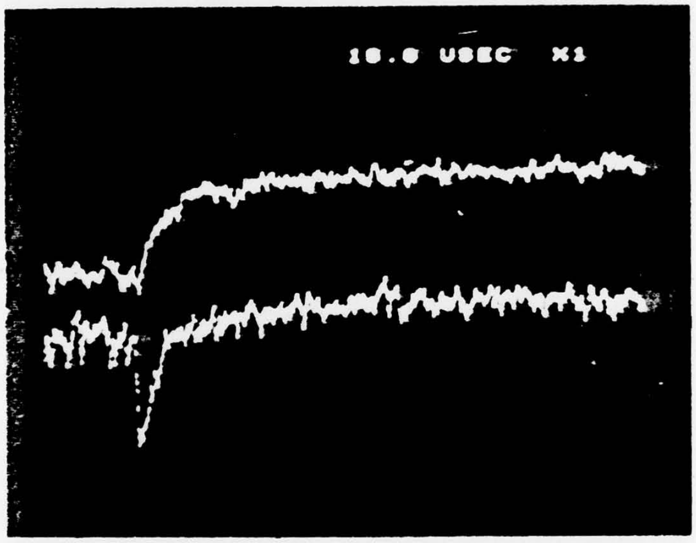
10.0 USEC X1

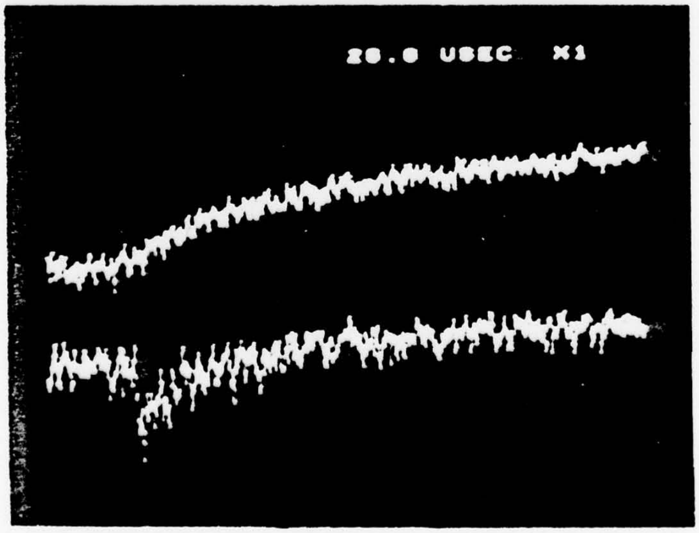
20.0 USEC X1

diminishes rapidly with attenuation of the CO_2 laser pulse. Figure 9 shows the relative fluorescence intensity as a function of the number of CO_2 laser photons absorbed. Points (2) and (3) are discussed further in the next section.

B. Comparison with Theory

In this experiment a mixture of ground and metastable triplet biacetyl molecules is irradiated with the CO_2 laser. We cannot easily determine whether the triplet states are directly excited by the infrared photons, or whether vibrational energy is initially deposited in electronically unexcited molecules. At the pressures at which these experiments were conducted, however, there should be rapid V-V equilibrium between the two electronic states. Since the vibrational structures of both states are very similar,[17] such V-V processes should be facilitated.

In order to interpret our results we make the following assumptions:

(a) The vibrational distributions of the ground and triplet electronic states are equilibrated in a time short compared with the characteristic decays of the induced fluorescence and phosphorescence signals.

(b) The vibrational distribution is characterized by a temperature.

(c) The translational and rotational temperatures of the vibrationally excited biacetyl molecules equilibrate rapidly with the vibrational temperature. This rapid relaxation is characteristic of polyatomic molecules with several thousand cm^{-1} of excess vibrational energy.[32,33] Furthermore, the low-frequency (45 cm^{-1}) torsional mode of biacetyl should have a very short V-R, T relaxation time,[34] and could be the principal channel for vibrational energy transfer.

Equations (15) and (16) of Chapter II account quantitatively for changes in the observed decay times and fluorescence amplitudes induced by infrared excitation. The calculations are carried out in four steps:

(1) The mean molecular energy, $\langle E\rangle$, following the CO_2 laser pulse is calculated from the relation

$$\langle E\rangle = \langle E\rangle_o + \langle n\rangle \qquad (18)$$

where $\langle E\rangle_o$ is the mean energy per biacetyl molecule at the initial temperature (300°K) prior to the laser pulse, and $\langle n\rangle$ is the mean number of CO_2 photons (1 photon = 944.2 cm^{-1}) absorbed per biacetyl molecule (as determined from equation (17)).

(2) The average molecular energy, $\langle E\rangle$, is related to the inverse temperature parameter, β, through the expression,

$$\langle E\rangle = \frac{1}{Z}\int_o^{\infty} E\,\rho(E)\,e^{-\beta E}\,dE + 3\beta^{-1} \qquad (19)$$

The second term in equation (19) accounts for the translational and rotational energy content, with the classical value of $\frac{1}{2}\beta^{-1}$ being assigned to each degree of freedom. The Haarhoff[35] expression for the vibrational density of states has been used for $\rho(E)$. The normal mode frequencies required in this calculation are the same as those used by van der Werf et al.[12] (see Appendix B). Since the majority of the molecules absorbing the CO_2 laser radiation are ground state singlet molecules, $\rho(E)$ should be the density of states for the ground electronic state. However, based on the normal mode frequencies available to us there is no major difference between the ground state, ^1A_g, and the excited triplet state, ^3A_u, densities of states (excluding constant terms), so the same values are used for both. The integration in equation (19) was done numerically on the PDP-8/L computer using the Extended Simpson's Rule.[36] Figure 7 shows a plot of the inverse temperature parameter, β, as a function of the mean energy content per molecule or the number of CO_2 photons absorbed.

(3) The predicted decay times of the phosphorescence and fluorescence are calculated as a function of β using equation (15). The empirical relation (10) is used in the integration. The computed decay times are represented by the solid curve of Figure 8 as a function of β or $\langle n \rangle$. Qualitatively the changes in the experimental decay times over three orders of magnitude are explained by this semiempirical calculation. Good agreement with experiment is found for laser fluences corresponding to excitation up to $\langle n \rangle = 3$. At higher CO_2 laser fluences the experimental results deviate from the simple model of equation (15). This is treated in further detail later. The deviation of the solid curve from the filled in experimental point at $\beta = 4.8\text{x}10^3$ $(cm^{-1})^{-1}$ is most likely due to the

FIGURE 7 -- Inverse temperature parameter, β, vs. mean molecular energy or mean number of CO_2 laser photons absorbed per molecule. (<1> = 944.2cm^{-1})

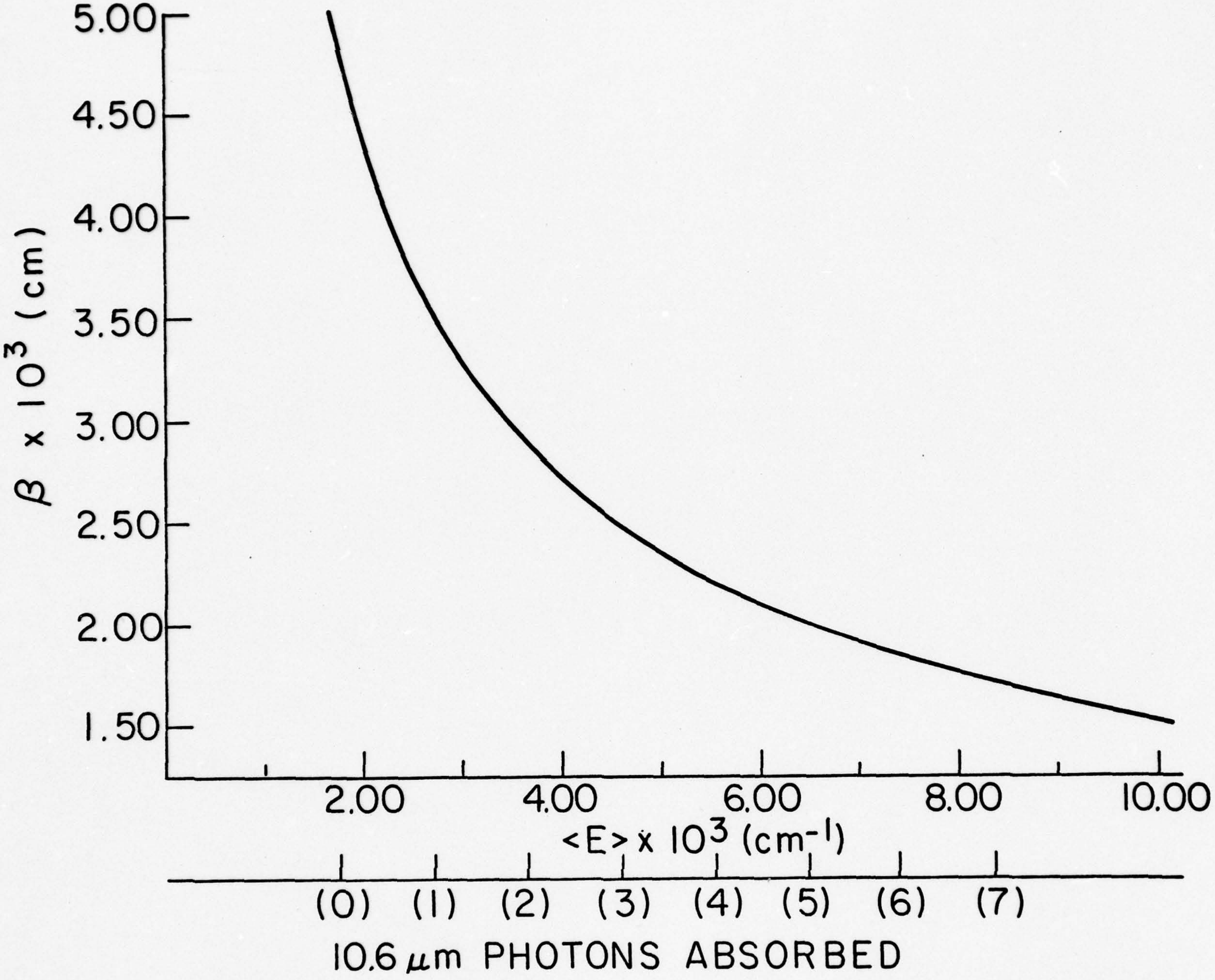
5.00
4.50
4.00
3.50
3.00
2.50
2.00
1.50
$\beta \times 10^3$ (cm)
2.00
4.00
6.00
8.00
10.00
<E> x 10^3 (cm^{-1})
(0)
(1)
(2)
(3)
(4)
(5)
(6)
(7)
10.6 μm PHOTONS ABSORBED

FIGURE 8 -- Biacetyl luminescence decay times vs. inverse temperature parameter, β, or mean number of CO_2 laser photons absorbed per molecule. ($<1> = 944.2 cm^{-1}$). The solid point in the upper left-hand corner is the unperturbed decay time of triplet biacetyl.[13] Circles represent experimental points.

——— Equation (15)
- - - Equation (26), $k = 1 \times 10^9 sec^{-1}$
-·-·- Equation (26), $k = 1 \times 10^8 sec^{-1}$
..... Equation (26), $k = 2 \times 10^7 sec^{-1}$

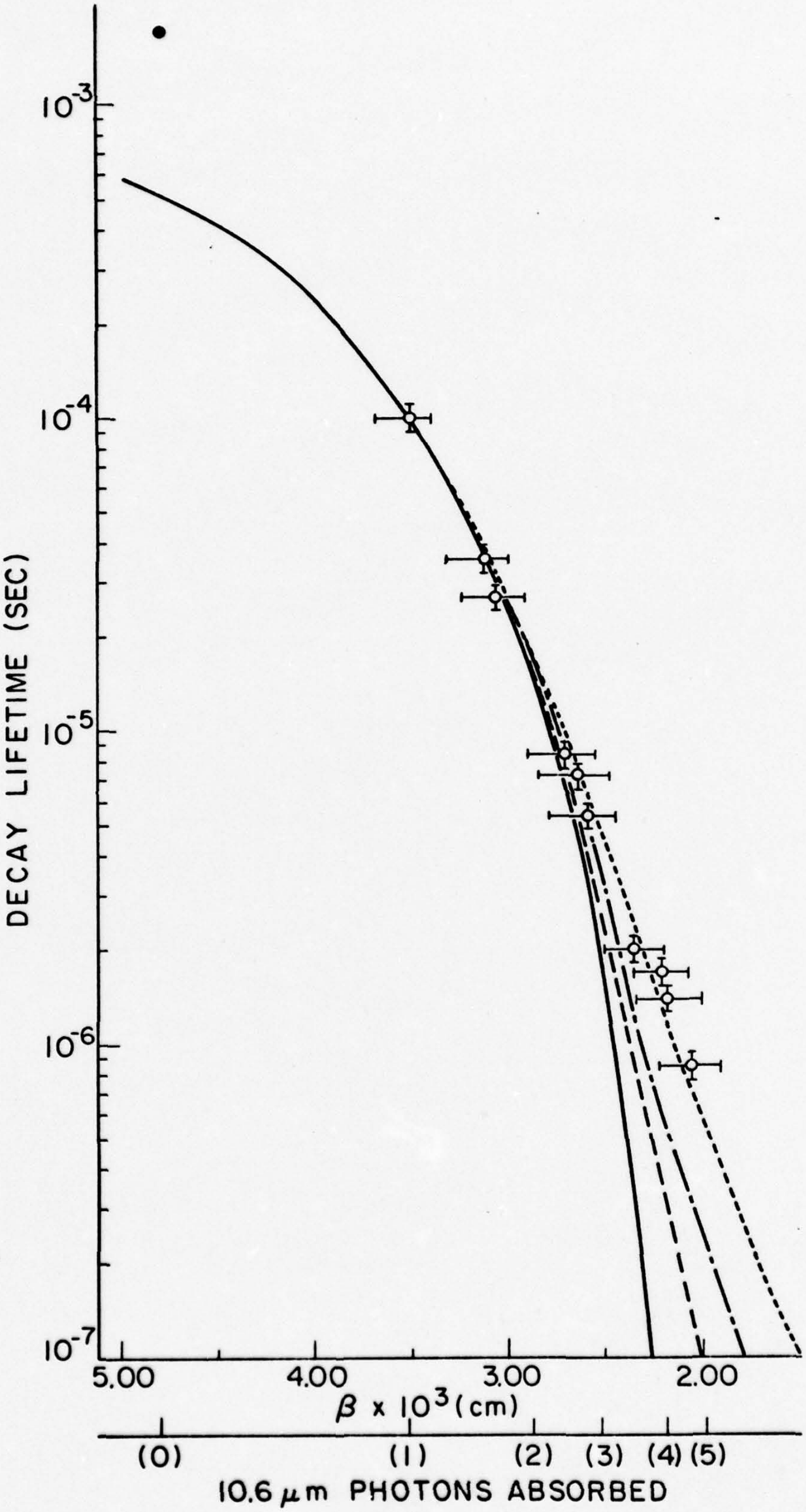
DECAY LIFETIME (SEC)
10^{-3}
10^{-4}
10^{-5}
10^{-6}
10^{-7}
5.00
4.00
3.00
2.00
$\beta \times 10^3$ (cm)
(0)
(1)
(2)
(3)
(4)
(5)
10.6 μm PHOTONS ABSORBED

FIGURE 9 -- Fluorescence emission amplitude vs. inverse temperature parameter, β, or mean number of CO_2 laser photons absorbed per molecule. (<1> = 944.2). Solid line is $e^{-\beta E_{ST}}$.

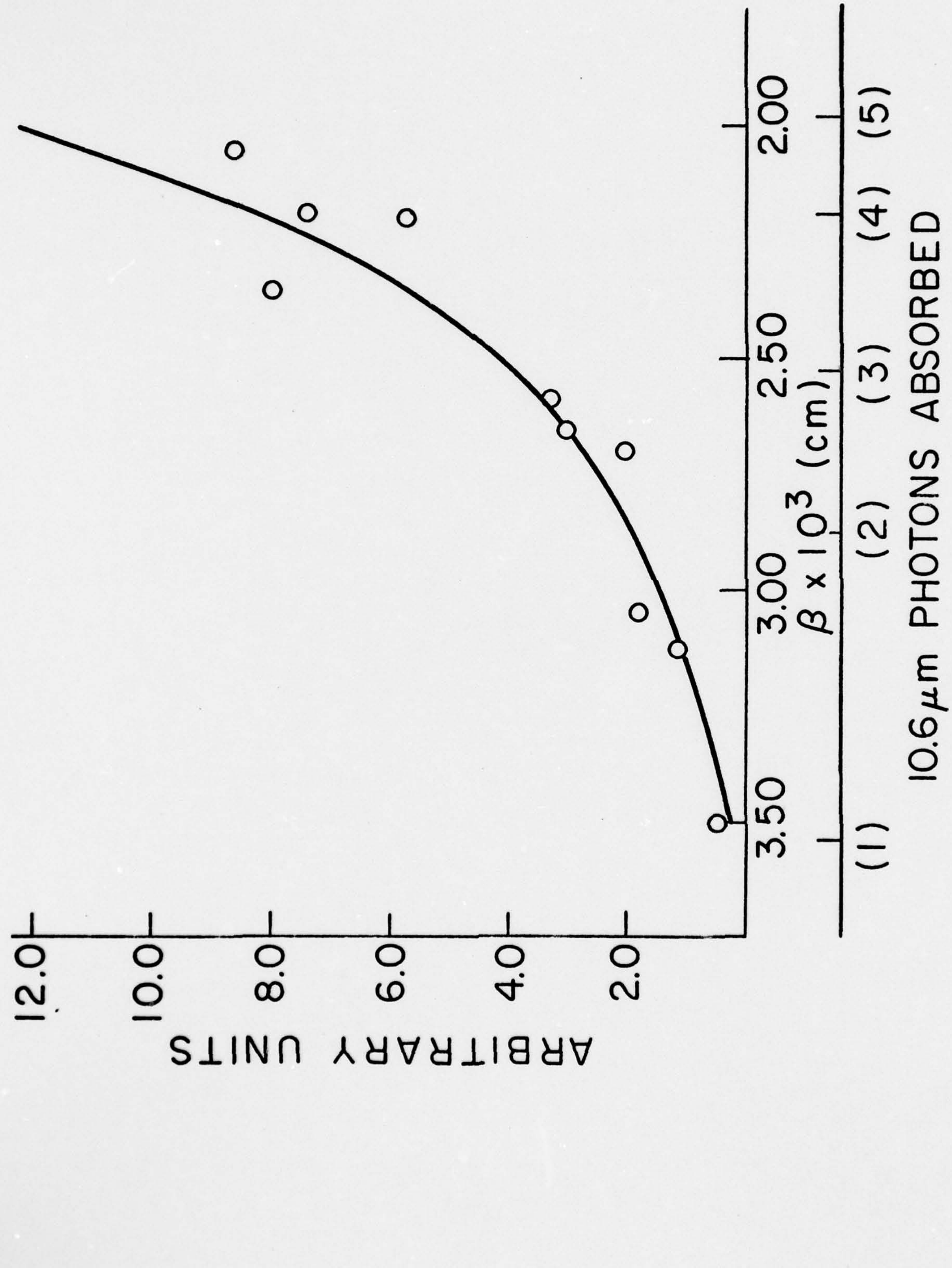
ARBITRARY UNITS
12.0
10.0
8.0
6.0
4.0
2.0
3.50
3.00
2.50
2.00
β x 10³ (cm)
(1)
(2)
(3)
(4)
(5)
10.6 μm PHOTONS ABSORBED

failure of the Haarhoff formula to accurately predict the density of vibrational states at very low vibrational energies.

(4) The predicted relative fluorescence signal amplitudes are calculated from equation (16) which predicts an exponential temperature dependence for A_F. As shown in Figure 9 the observed and predicted amplitudes are in close agreement.

An explanation of the deviation between the experimental and predicted decay times (Figure 8) at excitations greater than <n> = 3 lies in the deviation of the vibrational populations from a purely thermal distribution. The validity of equation (13) requires an infinitely fast coupling between the ground-state molecules and the excited triplets. Since the rate of this coupling is finite, the equation of motion of excited vibronic populations should be described in terms of a complicated master equation which takes all of the relaxation times into account. A simplified model, giving a qualitative explanation of these effects, will be presented instead.

We begin by rewriting Equation (13) as

$$\frac{dn(E)}{dt} = -\gamma_n(E)\ n(E) - k\ n(E) + \frac{k}{Z} N\ \rho_n(E)\ e^{-\beta E} \qquad (20)$$

The last two terms in equation (20) represent the interaction between the electronically excited levels and the bath. The term k n(E) gives the dissipation rate of an electronically excited molecule with vibrational energy E into all other vibronic levels through processes of the type:

$$BA^*(E) + BA \xrightarrow{k} BA^*(E') + BA \qquad (21)$$

where BA and BA* represent ground and electronically excited molecules respectively. In order to simplify the model it is assumed that k is independent of E, E' and the vibrational energy of the ground state molecule. Triplet-triplet energy transfer processes are neglected. The last term of equation (20) represents the filling of the level E from all other vibrational levels E'. This rate equation (equation (20)) reduces to the correct thermal equilibrium expression in the absence of the loss term $\gamma(E)\ n(E)$. When $n(E)$ reaches its thermal equilibrium value, $N\ Z^{-1}\ \rho_n(E)\ e^{-\beta E}$, the sum of the last two terms in equation (20) becomes zero and equation (13) is recovered.

The excited vibronic level decay kinetics can be discussed in two limiting cases.

(a) $\gamma_n(E) << k$. In this limit $n(E)$ retains its thermal equilibrium value given by equation (13).

(b) $\gamma(E) >> k$. In this limit the vibrationally excited molecules decay faster than they can be replenished and the rate of disappearance of the electronically excited population is determined by the slowest process taking place, which is the filling rate. Using the steady state approximation in equation (20) results in the following expression for $n(E)$:

$$n(E) \simeq \frac{k\ N}{Z\gamma_n(E)}\ \rho_n(E)\ e^{-\beta E} \qquad (22)$$

An approximate solution for the set of equations (20) can be described in the following way. We define an effective energy E_{eff} such that

$$\gamma_n(E_{eff}) = k \tag{23}$$

and divide the entire energy range into two regions. In region (a) $E < E_{eff}$ and n(E) is determined by equation (13). In region (b) $E > E_{eff}$ and n(E) is determined by equation (20). The rate equation for the entire electronically excited population becomes

$$\frac{dN}{dt} = \frac{d}{dt}\int_0^\infty n(E)\,dt = -\int_0^{E_{eff}} \gamma_n(E)\,n^a(E)\,dE - \int_{E_{eff}}^\infty \gamma_n(E)\,n^b(E)\,dE \tag{24}$$

The basis of this approximation is the substitution of $n^a(E)$ from equation (11) and $n^b(E)$ from equation (22) in the first and second integrals of equation (24), respectively. As a result, equations (14) and (15) are modified to give,

$$\frac{dN}{dt} = -\langle\gamma\rangle' N \tag{25}$$

$$\langle\gamma\rangle' = \frac{1}{Z}\left[\int_0^{E_{eff}} \gamma_n(E)\,\rho_n(E)e^{-\beta E}dE + k\int_{E_{eff}}^\infty \rho_n(E)\,e^{-\beta E}dE\right] \tag{26}$$

This approximation is equivalent to the model shown schematically in Figure 10. T and G represent the electronically excited and ground states, respectively. T_a and T_b are the

FIGURE 10 -- Schematic model of vibronic level relaxation in high pressure gas phase.

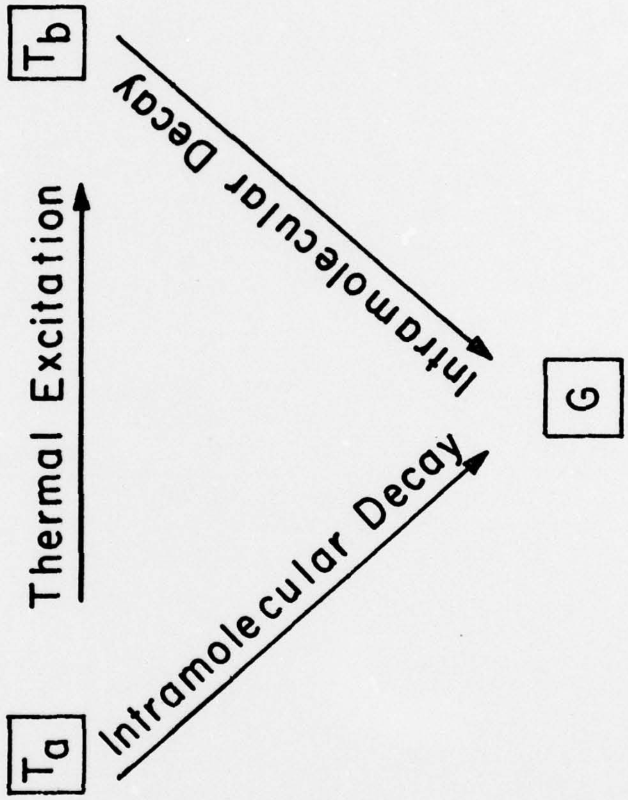
T_b
Thermal Excitation
Intramolecular Decay
G
Intramolecular Decay
T_a

vibronically excited molecules in region (a) and (b), respectively. Assuming that most of the vibronically excited population is in region (a), it follows that this population decays through two parallel channels. The first of these channels is the intramolecular decay and the second involves thermal excitation to region (b). The fast intramolecular decay rate characterizing region (b) prevents a reversible thermal deactivation to region (a). As mentioned above, a necessary condition for equation (24) to be valid is that the population of vibronically excited molecules in region (b) is small, or,

$$\int_{o}^{E_{eff}} \rho_n(E) e^{-\beta E} dE >> \int_{E_{eff}}^{\infty} \frac{k}{\gamma_n(E)} \rho_n(E) e^{-\beta E} dE \qquad (27)$$

By using the same arguments it can be shown that the expression (16) for the fluorescence intensity should be modified to be,

$$I_f = \left[\frac{1}{3} N\gamma_s^{rad} e^{-\beta E_{st}}\right] f(\beta) \qquad (28)$$

where the correction factor f(β) is given by

$$f(\beta) = \frac{\int_{o}^{E_{eff}} \rho_n(E)\ e^{-\beta E}\ dE}{\int_{o}^{\infty} \rho_n(E)\ e^{-\beta E}\ dE} \qquad (29)$$

Only thermally distributed molecules in region (a) contribute to the fluorescence intensity. Molecules excited to region (b) decay radiationlessly before they can emit a photon.

The decay curves corresponding to various values of k are plotted in Figure 8. The deviations of the experimental results from the solid curve at high fluences are qualitatively explained. The experimental data is best represented by a curve corresponding to $k = 2x10^7$ sec^{-1} which corresponds to an inverse relaxation rate, $(P_\tau)^{-1} = 4x10^6$ sec^{-1} $Torr^{-1}$. This value is reasonable for the resonant V-V transfer between the ground and excited vibronic states. From this treatment one would expect that for high CO_2 laser fluences the observed decay times would decrease if the biacetyl pressure were increased while keeping all other conditions (i.e. CO_2 laser fluence) the same. This effect was qualitatively observed when biacetyl pressure was increased from 5 to 10 Torr.

The dependence of the amplitude of the fluorescence signal on the temperature is deduced from equation (16) or (28). In Figure 9 $e^{-\beta E_{ST}}$ is plotted versus β and compared with the normalized experimental results. Since the correction due to f(β) in equation (28) is always less than 5%, it was neglected.

C. Effects of Added Buffer Gases

A qualitative study of buffer gas effects has been carried out. Addition of nonabsorbing gas to the biacetyl sample should result in decreasing the vibrational temperature of the biacetyl molecules due to the heat capacity of the buffer gas. This has been confirmed for biacetyl mixtures with argon or ethane. Addition of 5 Torr of ethane to 5 Torr of biacetyl results in a large increase in decay time. For instance, a decay time of 2 μsec was increased to 20 μsec. At the same CO_2 laser fluence about 60 Torr of argon is required to produce the same effect. Quantitative calculation should take into account the increased absorption of biacetyl-buffer gas mixtures with respect to pure biacetyl at the same partial pressure. For example, the addition of 100 Torr of argon to 10 Torr of biacetyl results in a 100% increase in absorption.

V. CONCLUSIONS

In this work we have shown that vibrational excitation of metastable triplet biacetyl molecules leads to changes in luminescence lifetimes and yields which are in complete agreement with current theories of radiationless processes. Furthermore, we have shown that vibrational excitation of triplet molecules produces the same luminescence features as vibrational excitation of singlet state molecules.[12] The end result of the two excitation methods is essentially equivalent. The vibrational energy distributions characteristic of the molecules taking part in these processes are best described as nearly thermal. Similar results could be expected for other "intermediate case" molecules.

In the past few years, multiple-photon absorption of intense CO_2 laser pulses and the subsequent dissociation of polyatomic molecules has been the subject of numerous investigations.[37] The primary diagnostic for such processes is, in general, the dissociation yield of the laser induced reaction. Occasionally the luminescence,[38] mass,[39] or translational energy[40] spectrum of the products is observed. Very few methods are available which are directly sensitive to the distribution of vibrational energy in the laser-excited molecule. The technique described here, when applicable, offers a convenient and sensitive probe for such vibrational energy distributions.

VI. APPENDICES

A. Variable Delay Unit

In order to trigger the CO_2 laser at a controlled delay following the mechanical shut-off of the visible laser beam a variable delay unit was constructed. A schematic diagram of this circuit is shown in Figure 11.

The operation of this unit is as follows. A small portion of the visible laser beam is reflected from a glass lens behind the chopper blade and focussed onto a phototransistor (A). When the chopper cuts off the light the bias of the phototransistor is changed. The unit responds by putting out a pulse at its output (B). The pulse is approximately +10v in amplitude (50Ω load) and .5 msec in duration. The pulse repetition rate is controlled by a potentiometer (C) and can be varied from .3 to 2 Hz independently of the chopping frequency.

The delay portion of the circuit, activated by a toggle switch (D), permits the addition of a controlled delay between the shut-off of the visible laser and the output pulse. The minimum delay time of the circuit (with switch (D) closed) is 1.6 μsec. When the delay portion of the circuit is connected in (switch (D) open) delays of between 12 μsec and 150 μsec can be obtained by varying the capacitance (E) and resistance (F) of the circuit. Addition of an auxiliary 1 μF capacitor (G) permits selection of delays between 200 and 320 μsec. Longer delays have been achieved by putting the output of the variable delay unit into a General Radio 1340 pulse

FIGURE 11 -- Schematic circuit diagram of variable delay unit.

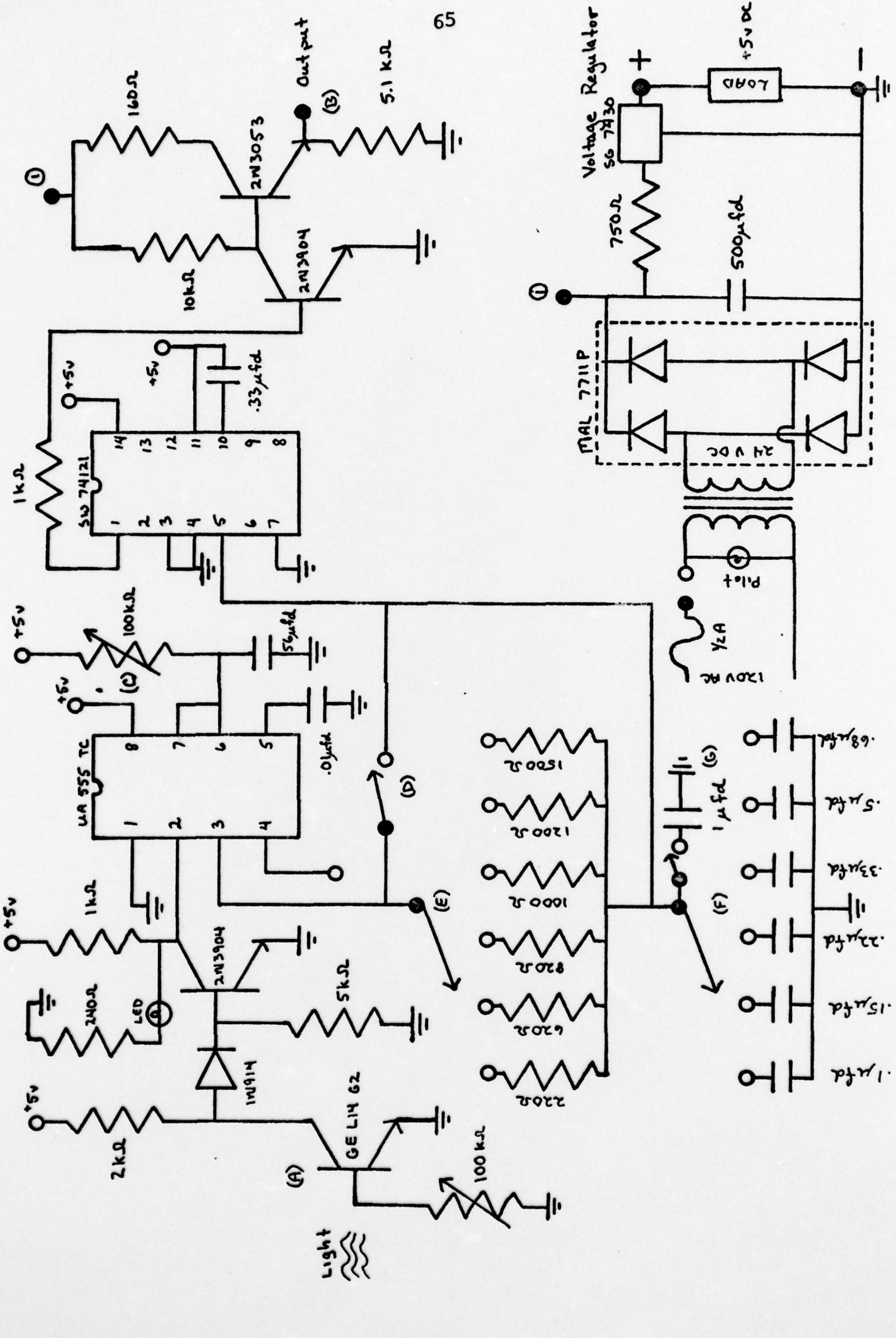
Light
(A)
GE L14 G2
100 kΩ
2 kΩ
+5v
1N914
LED
240Ω
2N3904
5kΩ
1kΩ
+5v
UA 555 TC
1
2
3
4
8
7
6
5
+5v
(C)
100kΩ
+5v
5μfd
.01μfd
(D)
(E)
220Ω
620Ω
820Ω
1000Ω
1200Ω
1500Ω
(F)
(G)
1μfd
.1μfd
.15μfd
.22μfd
.33μfd
.5μfd
.68μfd
SN 74121
1
2
3
4
5
6
7
14
13
12
11
10
9
8
1kΩ
+5v
+5v
.33μfd
2N3904
10kΩ
①
160Ω
2N3053
(B)
Output
5.1 kΩ
120V AC
1/2A
Pilot
24 V DC
MAL 7711P
①
750Ω
500μfd
Voltage Regulator
SG 7430
+
LOAD
+5v DC
−

generator. Precise calibration of the delays achieved by the variable delay unit is easily accomplished by monitoring the phototransistor response and the unit output on a dual-beam oscilloscope.

B. Density of States Calculation

In this work vibrational level densities were calculated with the Haarhoff formula.[35] This formula is,

$$N(E_v) = \left(\frac{2}{\pi s}\right)^{\frac{1}{2}} \frac{(1 - 1/12\ s)\lambda}{h\langle v\rangle\langle 1 + N\rangle} \left[(1 + \tfrac{1}{2}N)(1 + 2/N)^{\frac{1}{2}N}\right]^{s} \left[1 - 1/(1+N)^{2}\right]^{\beta o}$$

where $N(E_v)$ is the vibrational density of states, s is the number of normal modes (30 in the case of biacetyl) and the following definitions are made,

$$N = E_v/E_z$$

$$E_z = \sum_{i=1}^{s} \frac{1}{2} (h\ v_i)$$

$$\lambda = \prod_{i=1}^{s} (\langle v\rangle/v_i)$$

$$\beta_o = \frac{(s-1)(s-2)}{6s} \frac{\langle v^2\rangle}{\langle v\rangle^2} - \frac{s}{6}$$

For the ground state the normal mode frequencies suggested by van der Werf et al.[12] were used. These are: 2926, 2930, 2978, 2990, 3011, and 3018 (CH stretch); 1353, 1366, 1421, 1424, 1400, and 1400 (CH_3 deformations); 1111, 1274, 1052, and 1218 (CH_3 rocking); 257, 369, 534, and 685 (in-plane skeletal bend); 1718, 1719, 1004, 927, and 927 (in-plane skeletal stretch); 399 and 538 (out-of-plane skeletal deformations); 48 (central C-C torsion); 150 and 150 (CH_3 torsions).

Only little is known about the normal mode frequencies in both excited states. As suggested by van der Werf et al.[12] it was assumed that, in analogy to glyoxal, the only important frequency change occurs in the C-C torsional mode, a frequency increase by a factor of 1.8. Thus, neglecting the constant terms (which always cancelled out in our treatment) the ground and excited state densities of states were essentially the same.

C. Joulemeter Resurfacing

Pyroelectric energy meters, such as the Gentec ED-200 Joulemeter used in this experiment, rely on a layer of absorbing material on the detector head to provide rapid and uniform transfer of the incident radiant energy to the pyroelectric crystal. Prolonged usage or exceeding the maximum recommended incident energy (.5 joules per square centimeter in the case of the Gentec ED-200) with short, high peak power pulses can lead to a gradual deterioration of the detector surface. This is evidenced by the appearance (in the case of the ED-200) of grey areas on the detector head as the black absorbing coating is worn off. Such deterioration changes the responsivity of the detector, and recoating of the detector surface followed by recalibration is necessary. Most manufacturers (including Gentec) recommend factory servicing. However, when time is a factor detector resurfacing can be accomplished in the laboratory with good results. The following procedure was developed to resurface a Gentec ED-200 joulemeter. This procedure provides a detector surface which will hold up well for maximum energy densities of .5 Joules per square centimeter. For very low energy densities any absorbing coating such as Krylon flat black paint works well.

The procedure is as follows:

(1) Clean the detector surface by sanding lightly and wiping with a cloth soaked in a solvent such as acetone. Remove the existing black coating leaving a uniform surface.

(2) Check to see if the thin metallic layer which lies beneath the black absorbing coating is damaged. Damage is evidenced by a nonuniform coloring of the detector head. If the metallic layer is damaged cover the detector surface with a thin, uniform layer of silver print conducting paint (available from G.C. Electronics). Dry detector surface under a heat lamp for 1 hour.

(3) Paint over the silver print with a thin, uniform layer of printers ink (Speedball, oil-based works well). Thin the ink with acetone and apply with a small brush. Dry for 36 hours under a heat lamp.

(4) Recalibrate detector using either a radiation source of known intensity or by comparison with another calibrated detector.

REFERENCES

1. H. L. J. Bäckström and K. Sandros, Acta Chem. Scandinavica 12, 823 (1958).
2. J. T. Dubois and F. Wilkinson, J. Chem. Phys. 39, 899 (1963).
3. W. A. Noyes, Jr., W. A. Mulac, and M. S. Matheson, J. Chem. Phys. 36, 880 (1962).
4. G. F. Sheats and W. A. Noyes, Jr., J. Am. Chem.Soc. 77, 1421 (1955).
5. Two rather complete reviews are:
   a) W. A. Noyes, Jr., G. B. Porter, and J. E. Jolley, Chem. Revs. 56, 49 (1956);
   b) R. B. Cundall and A. S. Davies, Progr. Reaction Kinetics 4, 149 (1967).
6. C. S. Parmenter and H. M. Poland, J. Chem. Phys. 51, 1551 (1969).
7. (a) H. W. Sidebottom, C. C. Badcock, J. G. Calvert, B. R. Rabe, and E. K. Damon, J. Am. Chem. Soc. 94, 13 (1972);
   (b) C. C. Badcock, H. W. Sidebottom, J. G. Calvert, B. R. Rabe, and E. K. Damon, ibid. 94, 19 (1972).
8. G. M. McClelland and J. T. Yardley, J. Chem. Phys. 58, 4368 (1973).
9. A. Z. Moss and J. T. Yardley, J. Chem. Phys. 61, 2883 (1974).
10. E. Drent, R. P. van der Werf, and J. Kommandeur, J. Chem. Phys. 59, 2061 (1973).
11. R. van der Werf, D. Zevenhuijzen, and J. Kommandeur, Chem. Phys. Letts., 27, 325 (1974).
12. R. van der Werf and J. Kommandeur, Chem. Phys. 16, 125 (1976).
13. F. B. Wampler and R. C. Oldenberg, Intl. J. Chem. Kinetics (to be published).

14. M. Bixon and J. Jortner, J. Chem. Phys. 48, 715 (1968).

15. R. Van der Werf, D. Zevenhuijzen, and J. Jortner, Chem. Phys. 27, 319 (1978).

16. J. W. Sidman and D. S. McClure, J. Am. Chem. Soc. 77, 6461 (1955).

17. J. C. D. Brand and A. W. H. Mau, J. Am. Chem. Soc. 96, 4380 (1974).

18. E. Drent and J. Kommandeur, Chem. Phys. Lett. 14, 321 (1972).

19. J. W. Sidman and D. S. McClure, J. Am. Chem. Soc. 77, 6471 (1955).

20. J. R. Durig, S. G. Hannum, and S. C. Brown, J. Phys. Chem. 75, 1946 (1971).

21. A. Yogev and Y. Haas, Chem. Phys. Lett. 21, 544 (1973).

22. B. J. Orr, Chem. Phys. Lett. 43, 446 (1976).

23. F. Lahmani, A. Tramer, and C. Tric, J. Chem. Phys. 60, 4431 (1974).

24. A. Nitzan, J. Jortner, and P. M. Rentzepis, Proc. Roy. Soc. A327, 367 (1972).

25. M. Bixon and J. Jortner, J. Chem. Phys. 50, 4061 (1964).

26. An extensive review on the subject is:
K. F. Freed in Topics in Applied Physics, Vol. 15, pp 23-164, Springer-Verlag, New York, (1976).

27. C. Tric, Chem. Phys. Lett. 21, 83 (1973).

28. The rms diffusion length of biacetyl triplets is given as 3 mm at 0.6 torr[7a], and <x> scales as $p^{-1/2}$.

29. Computer program for exponential fit was supplied by Dr. Anthony Kotlar, Steinfeld Group, M.I.T.

30. For a description of the opto-acoustic apparatus, see F. M. Lussier, J. I. Steinfeld, and T. F. Deutch, Chem. Phys. Lett. in press.

31. C. A.Parker, "Photoluminescence in Solutions," Elsivier, Amsterdam, 1968.

32. D. C. Tardy and B. S. Rabinovitch, Chem. Rev. 77, 369 (1977).

33. C. C. Jensen, J. I. Steinfeld, and R. D. Levine, J. Chem. Phys. (in press).

34. J. D. Lambert and R. Salter, Proc. Roy. Soc. A253, 277 (1954).

35. P. C. Haarhoff, Mol. Phys. 7, 101 (1963).

36. M. Abramowitz and I. A. Stegun, Handbook of Mathematical Functions, Dover Publications, Inc., New York (1965) p. 886.

37. Two recent reviews are;

   a) C. D. Cantrell, S. M. Freund, and J. L. Lyman, in "Laser Handbook, Vol. III" (M. Stitch, ed), North-Holland, Amsterdam (1978).

   b) R. V. Ambartzumyan and V. S. Letokhov, in "Chemical and Biochemical Applications of Lasers, Vol. III" (C. B. Moore, ed), Academic Press, New York (1977).

38. D. S. King and J. C. Stephenson, Chem. Phys. Lett. 51, 48 (1977).

39. J. W. Hudgens, J. Chem. Phys. 68, 777 (1978).

40. Aa. S. Sudbo, P. A. Schulz, E. R. Grant, Y. R. Shen, and Y. T. Lee, J. Chem. Phys. 68, 1306 (1978).